Relativistic jets in GRB and neutron star mergers

Hendrik van Eerten

University of Bath, United Kingdom

Vulcano Workshop 2024 –
Frontier Objects in Astrophysics and Particle Physics
May 27, 2024

Science and Technology Facilities Council

Funded by the Horizon 2020
Framework Program
of the European Union
Grant Agreement No. 871158

Gamma-ray bursts and their afterglows (schematic)

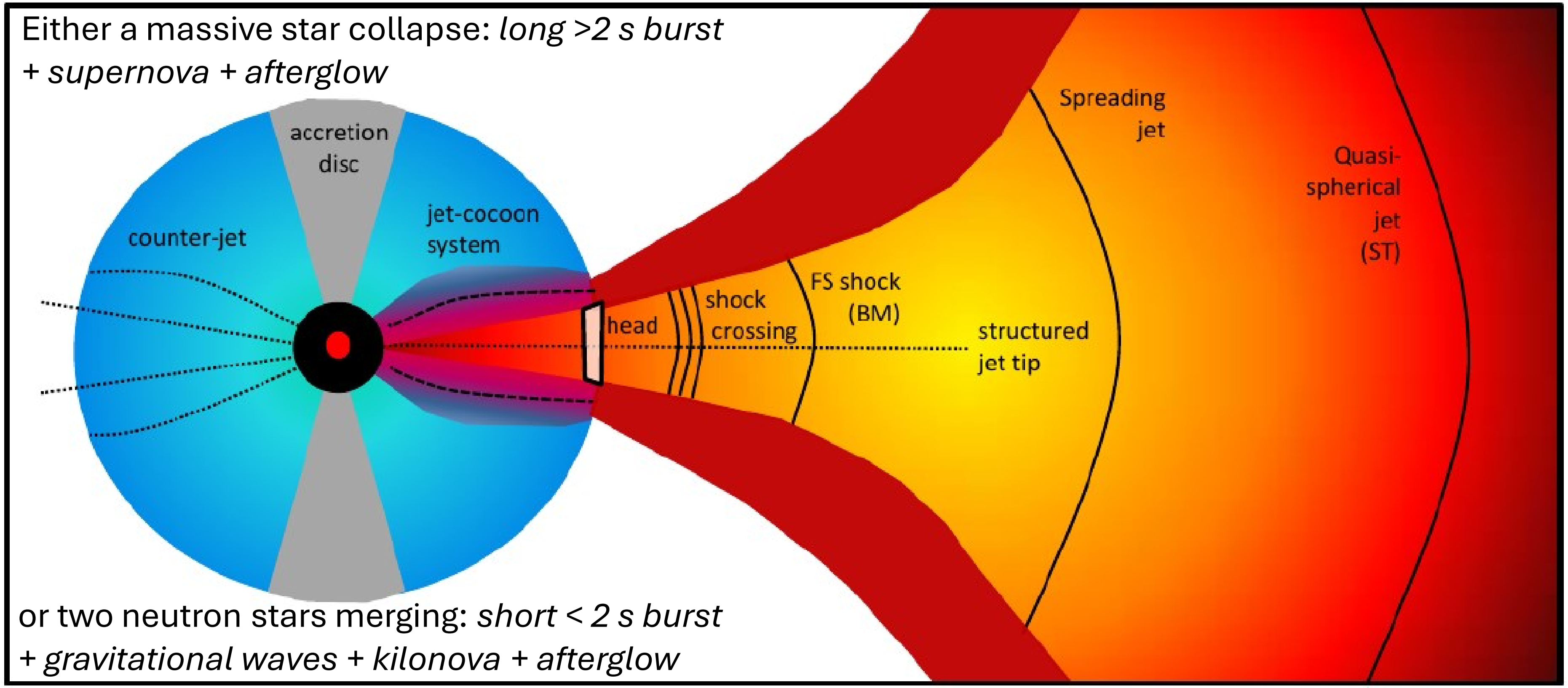

Either a massive star collapse: *long >2 s burst*
+ *supernova* + *afterglow*

or two neutron stars merging: *short < 2 s burst*
+ *gravitational waves* + *kilonova* + *afterglow*

IMG: Van Eerten

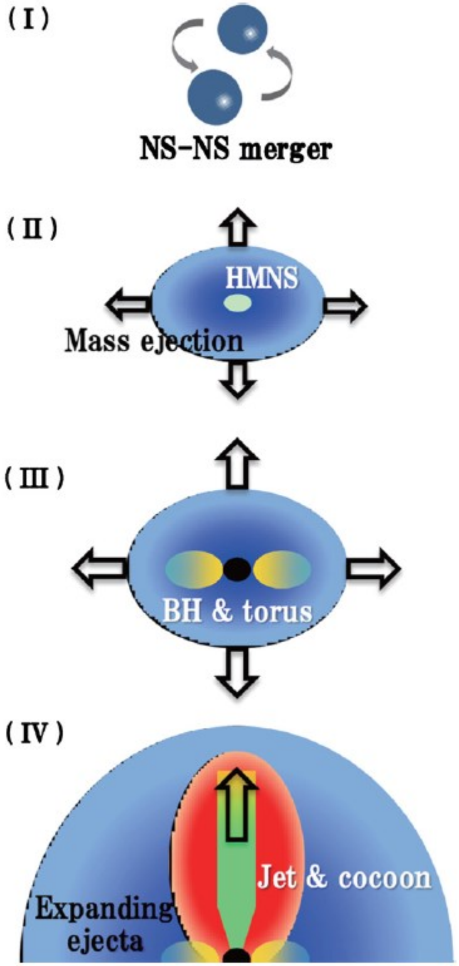

Nagakura+ 2014

Note, these *hydrodynamical* jets quickly evolve into *collisionless shocks/blast waves*

prompt and afterglow emission

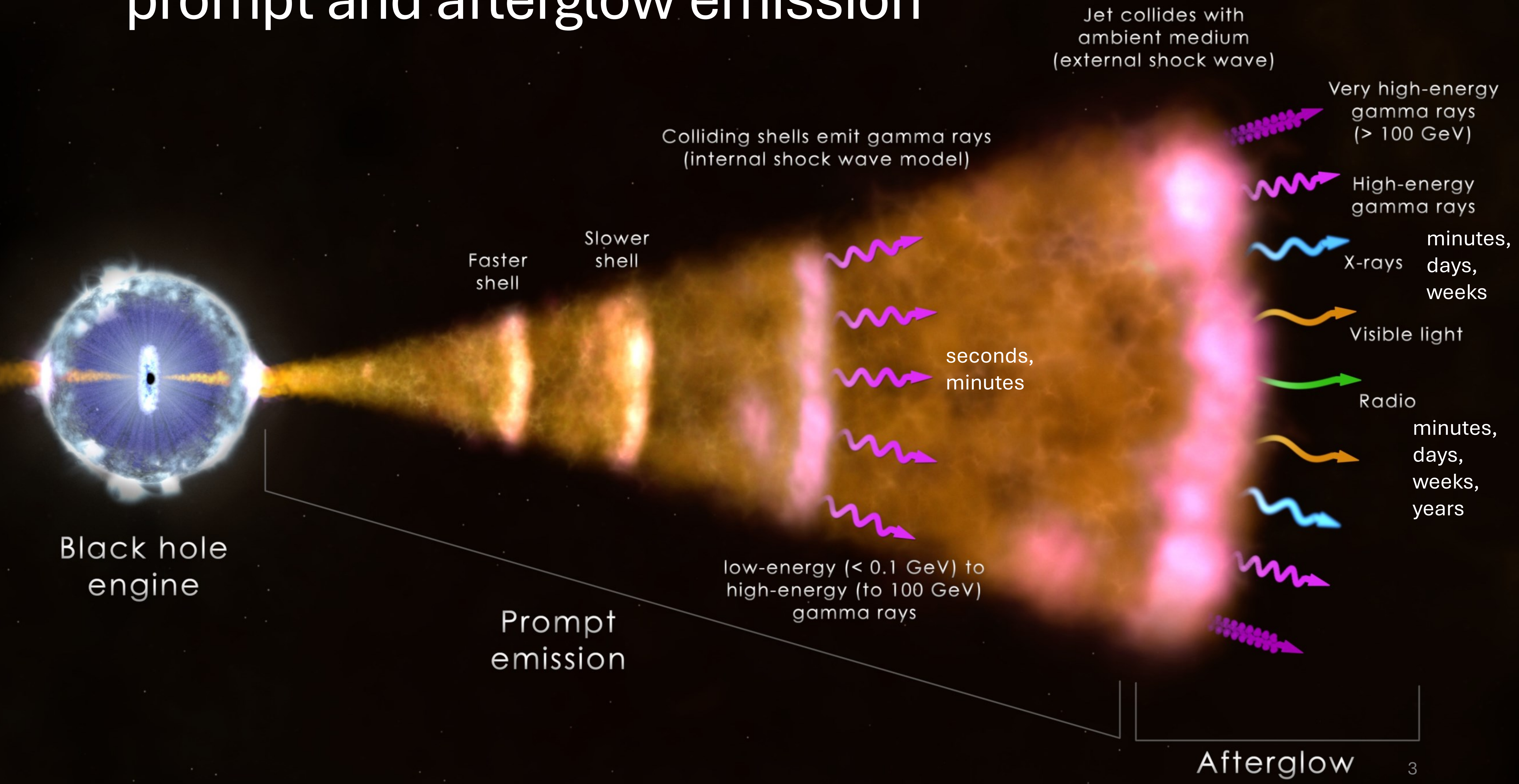

Illustrative animation of short GRB jet breaking out

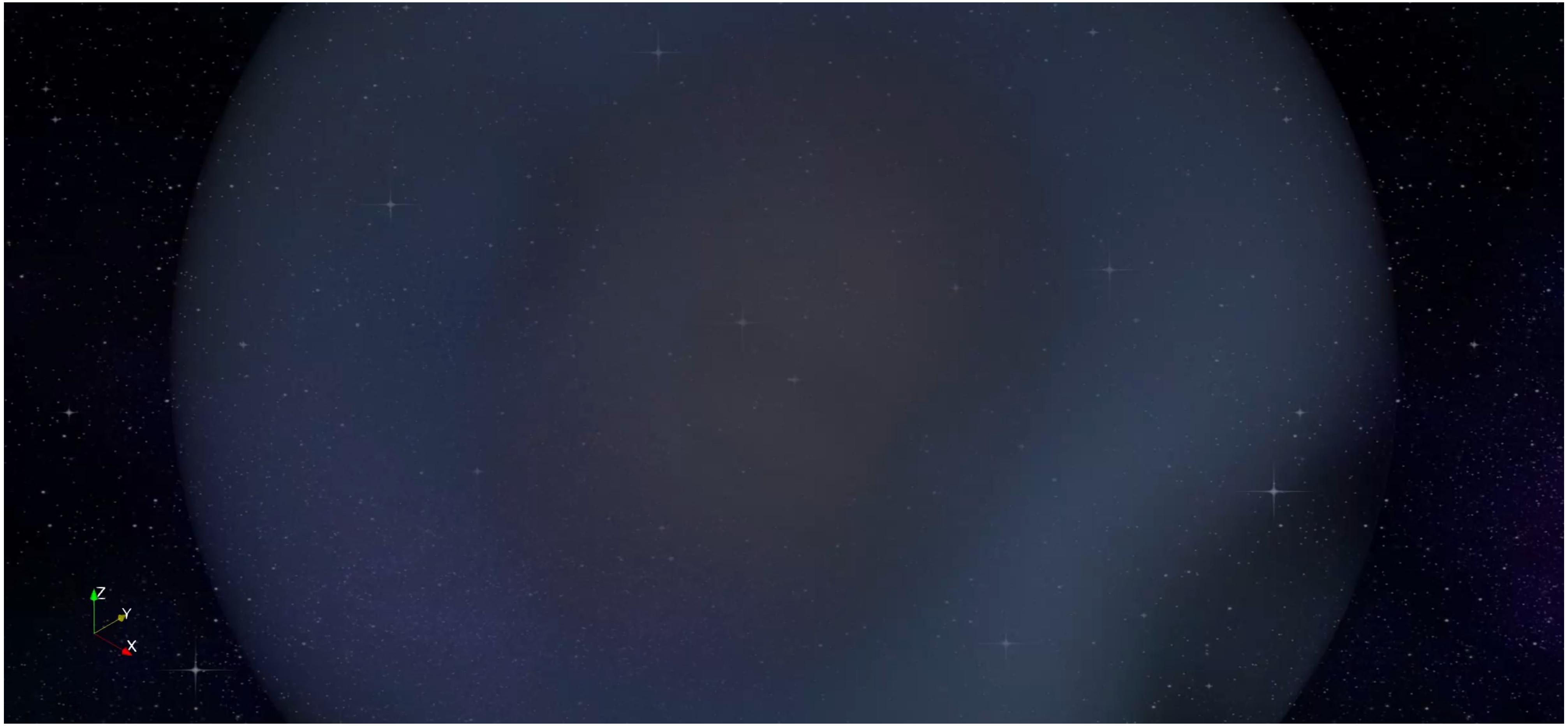

The neutrino-driven wind has shaped the jet, now to get past the dynamical ejecta scale & photosphere (around 1e12 cm)

Gottlieb+ 2022 ApJL 933, L2

moving mesh methods can follow the jet across afterglow scales

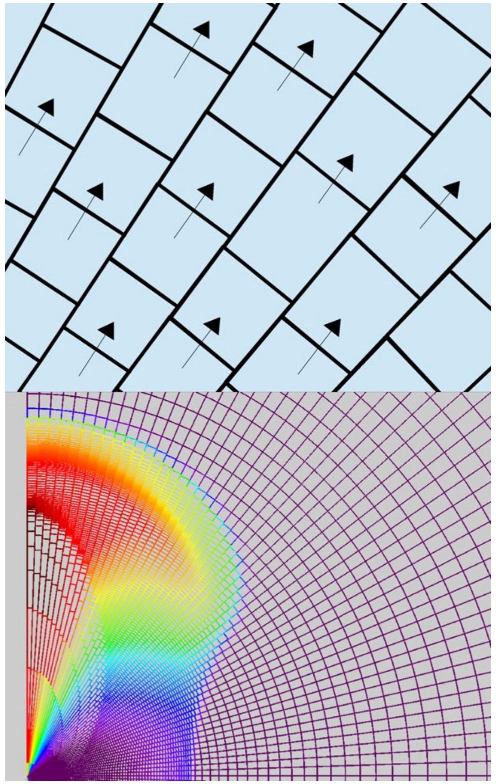

Duffell & MacFadyen 2013
Ayache, Van Eerten & Eardsley 2021

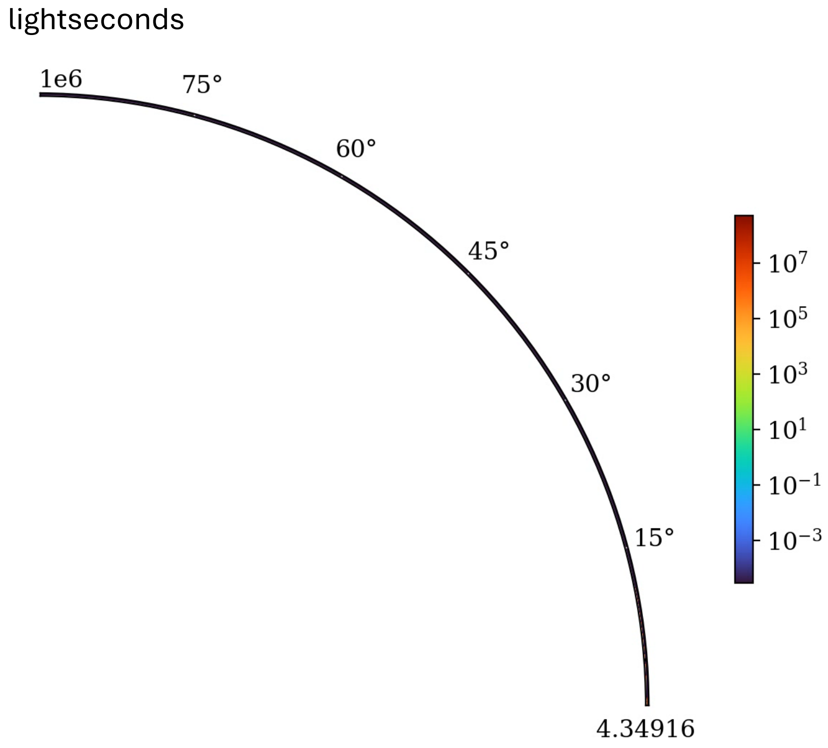

long-term evolution (> 1e15 cm) remains separate challenge
similar expansion behaviour found for various jet structures

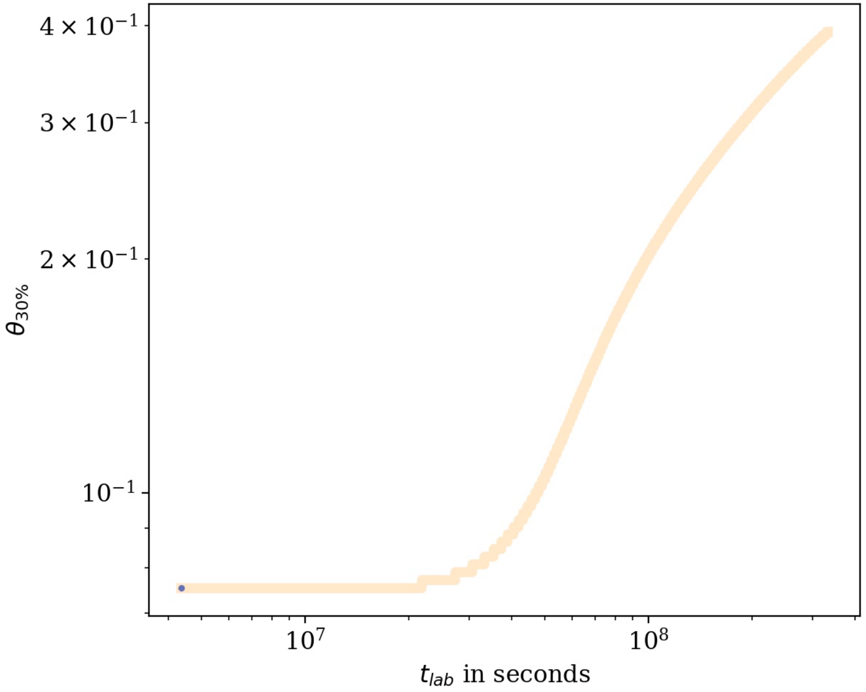

Kundu & Van Eerten (in prep)
(see also: Govreen-Segal+ 2023)

The full afterglow spectrum, including TeV emission

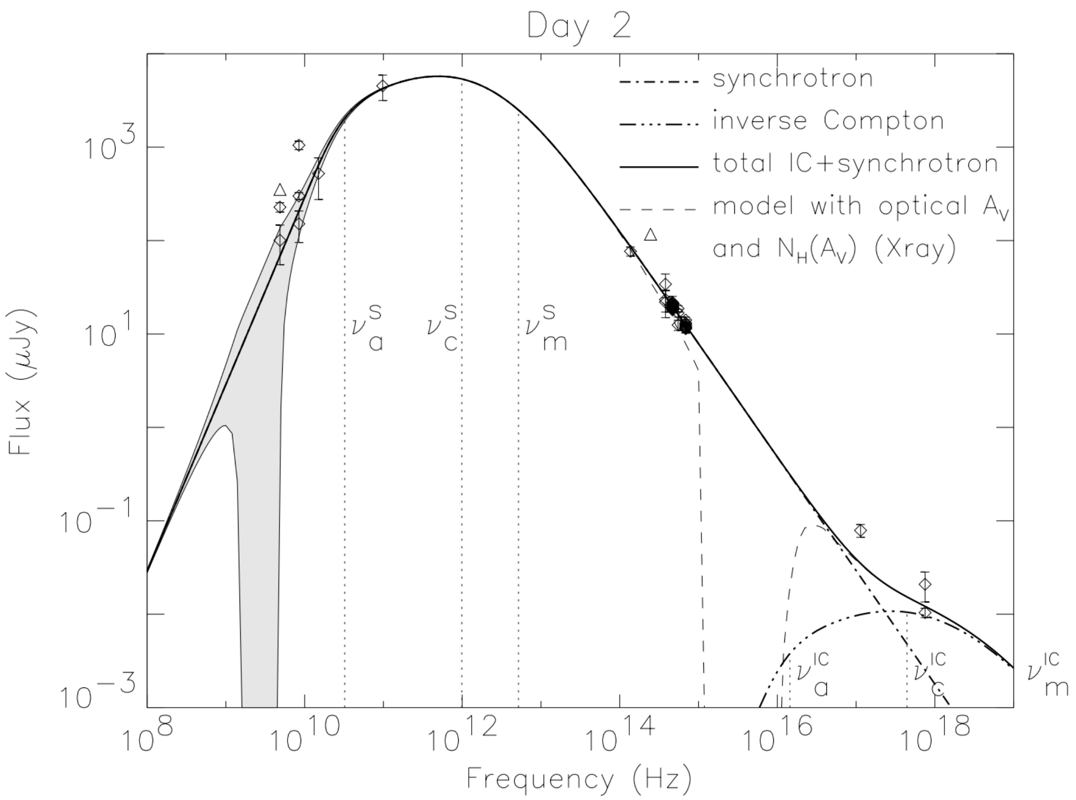

GRB 000926, Harrison et al. (2001)

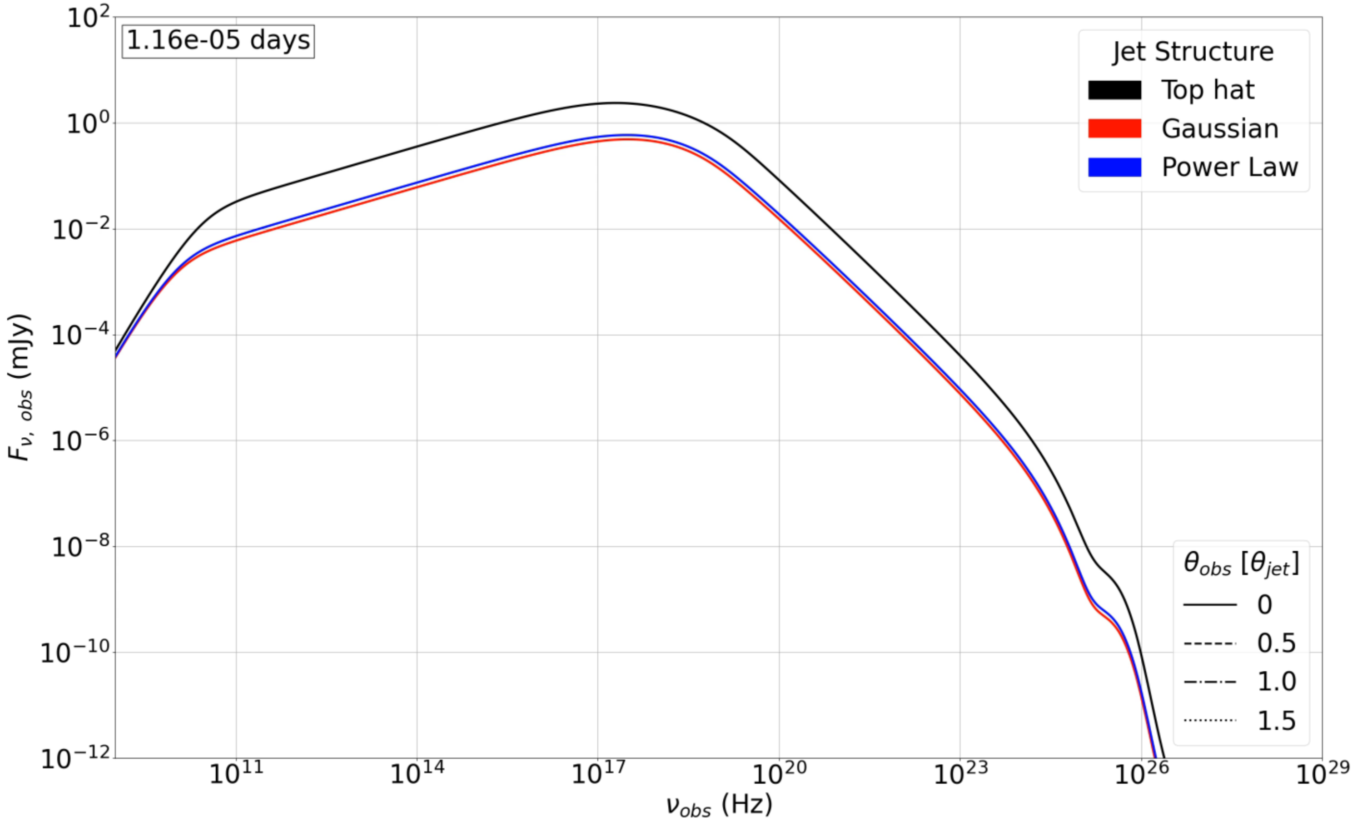

“generic” long GRB, Hope & Van Eerten (in prep.)

Based on full kinetic modelling of electron &
photon populations in energy space for multiple (structured jet) sites
Note synchrotron cut-off and Synchrotron self-Compton component,
the latter attenuated by extra-galactic background light (EBL)

What is currently happening in our field?

A list of noteworthy recent GRBs

- GRB 160821B. Short GRB with TeV emission.
- GRB 170817A. gravitational waves detected.
- GRB 180720B. HESS detected.
- GRB 190114C. TeV photons MAGIC.
- GRB 190829A. TeV photons.
- GRB 200826A. A short GRB from massive star collapse.
- GRB 201015A. TeV burst.
- GRB 201216C. MAGIC detected.
- GRB 210610B. 54 deg polarization angle rotation.
- GRB 211211A. long GRB from neutron star merger.
- GRB 221009A. brightest of all time.
- GRB 230307A. long GRB with a kilonova.
- GRB 240219A. Einstein Probe detection EP240219A.
- GRB 240315C. Einstein Probe detection.
- GRB 240402B. LEIA detection.

What is currently happening in our field?

A list of noteworthy recent GRBs

- GRB 160821B. Short GRB with TeV emission.
- GRB 170817A. gravitational waves detected.
- GRB 180720B. HESS detected.
- GRB 190114C. TeV photons MAGIC.
- GRB 190829A. TeV photons.
- GRB 200826A. A short GRB from massive star collapse.
- GRB 201015A. TeV burst.
- GRB 201216C. MAGIC detected.
- GRB 210610B. 54 deg polarization angle rotation.
- GRB 211211A. long GRB from neutron star merger.
- GRB 221009A. brightest of all time.
- GRB 230307A. long GRB with a kilonova.
- GRB 240219A. Einstein Probe detection EP240219A.
- GRB 240315C. Einstein Probe detection.
- GRB 240402B. LEIA detection.

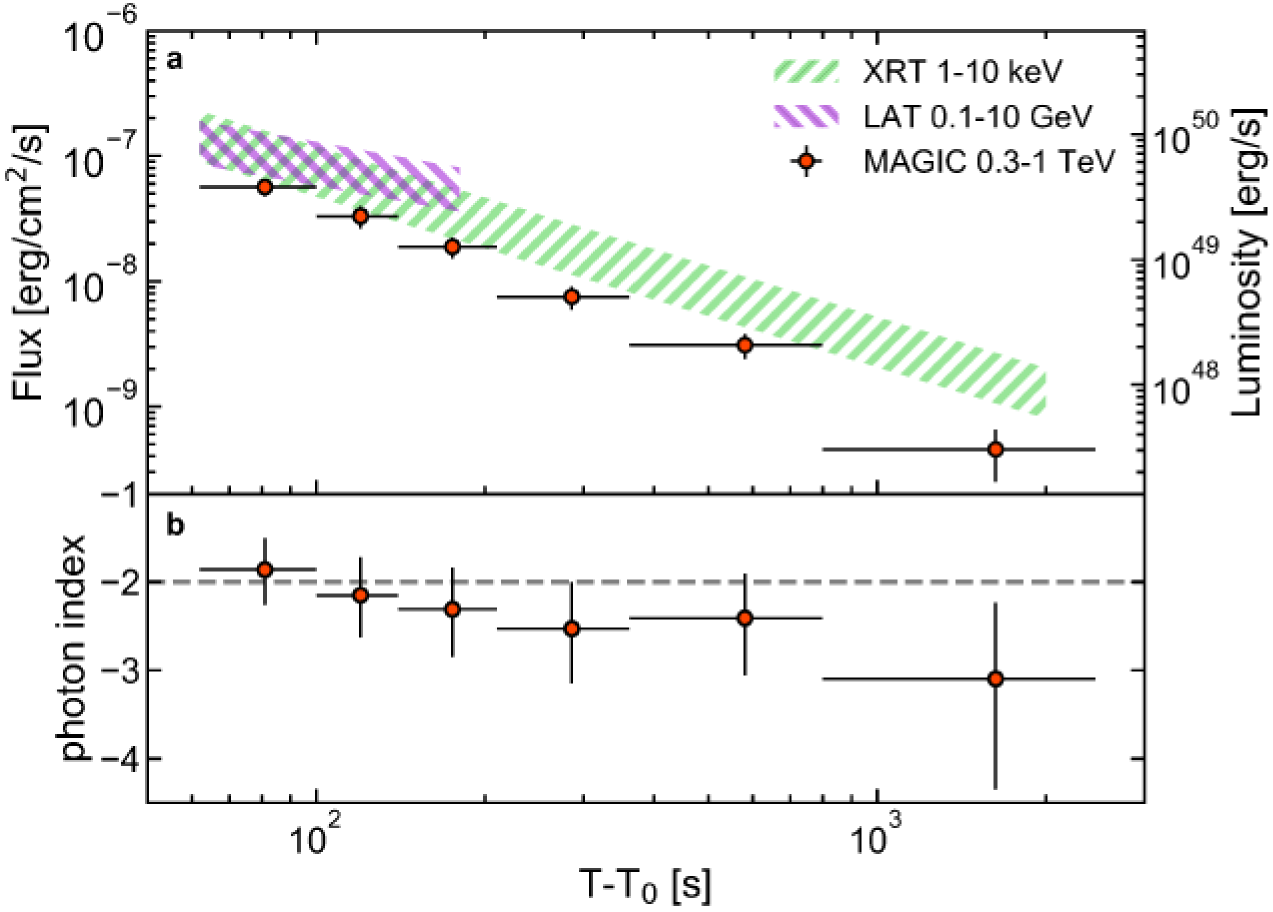

GRB 190114C. MAGIC 2020, Nature 575, 455

What is currently happening in our field?

A list of noteworthy recent GRBs

- GRB 160821B. Short GRB with TeV emission.
- GRB 170817A. gravitational waves detected.
- GRB 180720B. HESS detected.
- GRB 190114C. TeV photons MAGIC.
- GRB 190829A. TeV photons.
- GRB 200826A. A short GRB from massive star collapse.
- GRB 201015A. TeV burst.
- GRB 201216C. MAGIC detected.
- GRB 210610B. 54 deg polarization angle rotation.
- GRB 211211A. long GRB from neutron star merger.
- GRB 221009A. brightest of all time.
- GRB 230307A. long GRB with a kilonova.
- GRB 240219A. Einstein Probe detection EP240219A.
- GRB 240315C. Einstein Probe detection.
- GRB 240402B. LEIA detection.

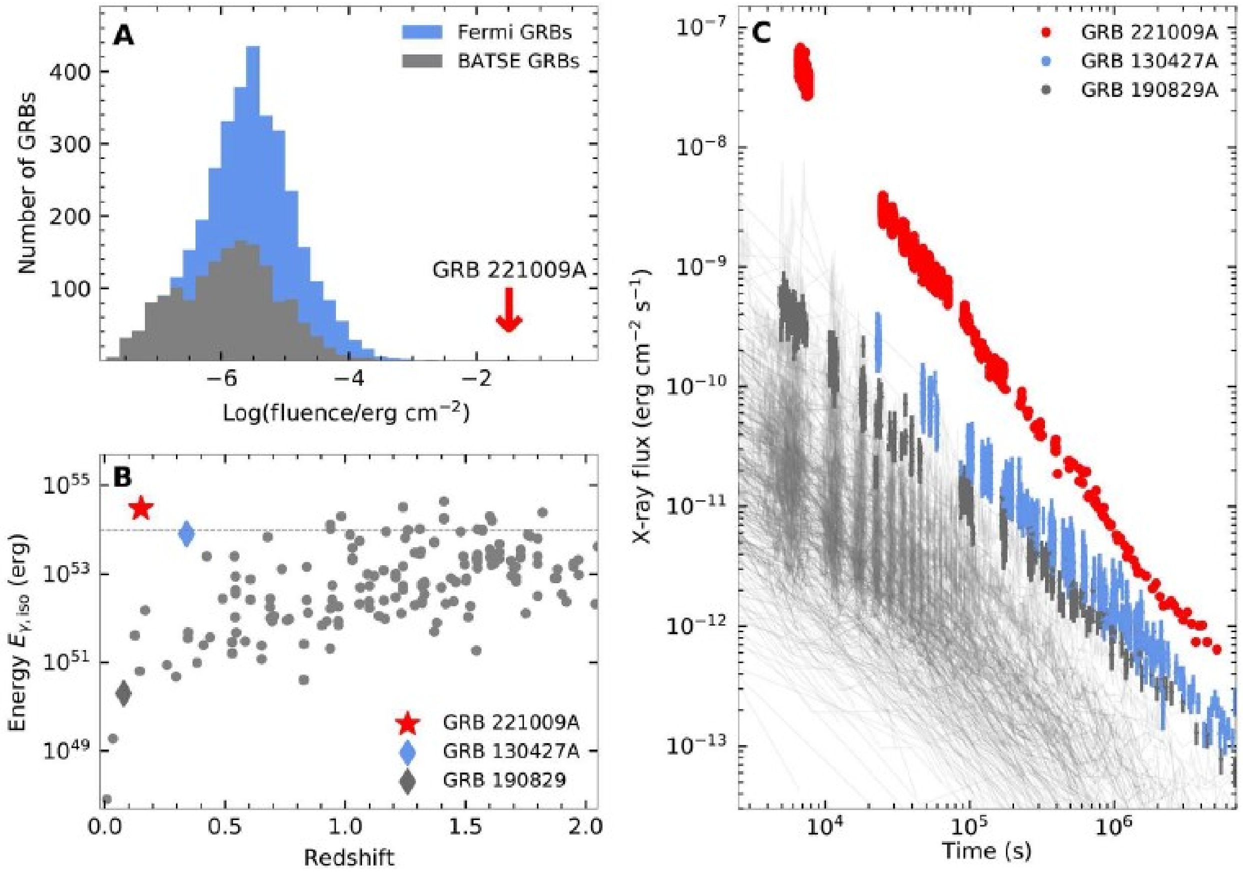

O'Connor+ 2023, Science Advances 9, 1405

What is currently happening in our field?

A list of noteworthy recent GRBs

- GRB 160821B. Short GRB with TeV emission.
- GRB 170817A. gravitational waves detected.
- GRB 180720B. HESS detected.
- GRB 190114C. TeV photons MAGIC.
- GRB 190829A. TeV photons.
- GRB 200826A. A short GRB from massive star collapse.
- GRB 201015A. TeV burst.
- GRB 201216C. MAGIC detected.
- GRB 210610B. 54 deg polarization angle rotation.
- GRB 211211A. long GRB from neutron star merger.
- GRB 221009A. brightest of all time.
- GRB 230307A. long GRB with a kilonova.
- GRB 240219A. Einstein Probe detection EP240219A.
- GRB 240315C. Einstein Probe detection.
- GRB 240402B. LEIA detection.

GRB 211211A

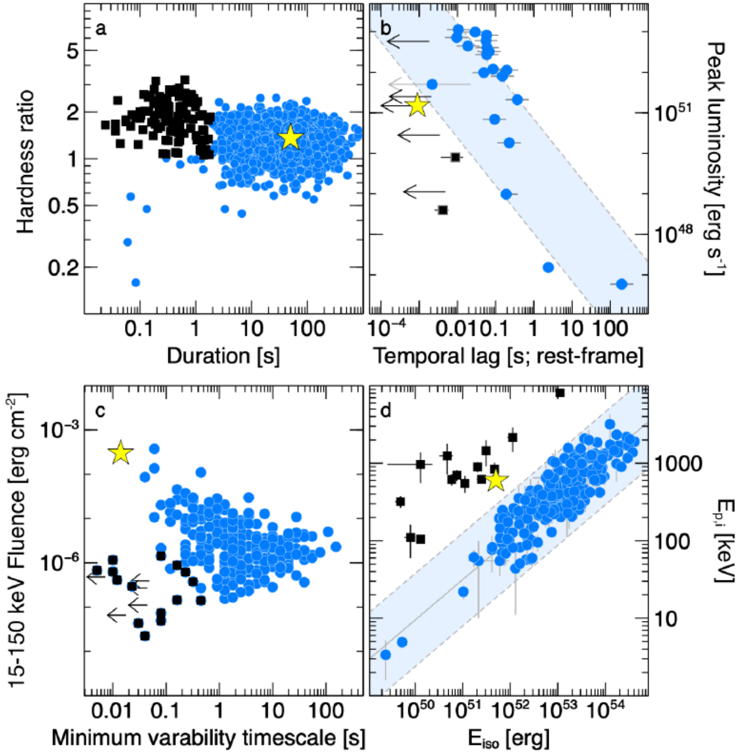

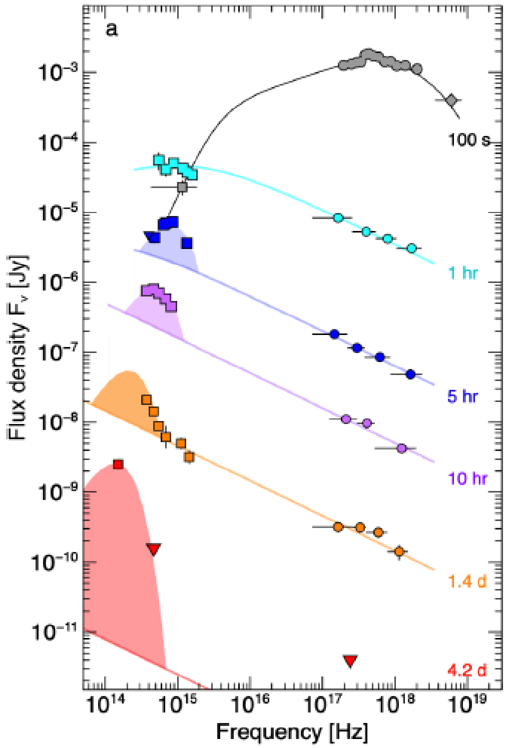

Troja+ 2022, Nature 612, 228

What is currently happening in our field?

A list of noteworthy recent GRBs

- GRB 160821B. Short GRB with TeV emission.
- GRB 170817A. gravitational waves detected.
- GRB 180720B. HESS detected.
- GRB 190114C. TeV photons MAGIC.
- GRB 190829A. TeV photons.
- GRB 200826A. A short GRB from massive star collapse.
- GRB 201015A. TeV burst.
- GRB 201216C. MAGIC detected.
- GRB 210610B. 54 deg polarization angle rotation.
- GRB 211211A. long GRB from neutron star merger.
- GRB 221009A. brightest of all time.
- GRB 230307A. long GRB with a kilonova.
- GRB 240219A. Einstein Probe detection EP240219A.
- GRB 240315C. Einstein Probe detection.
- GRB 240402B. LEIA detection.

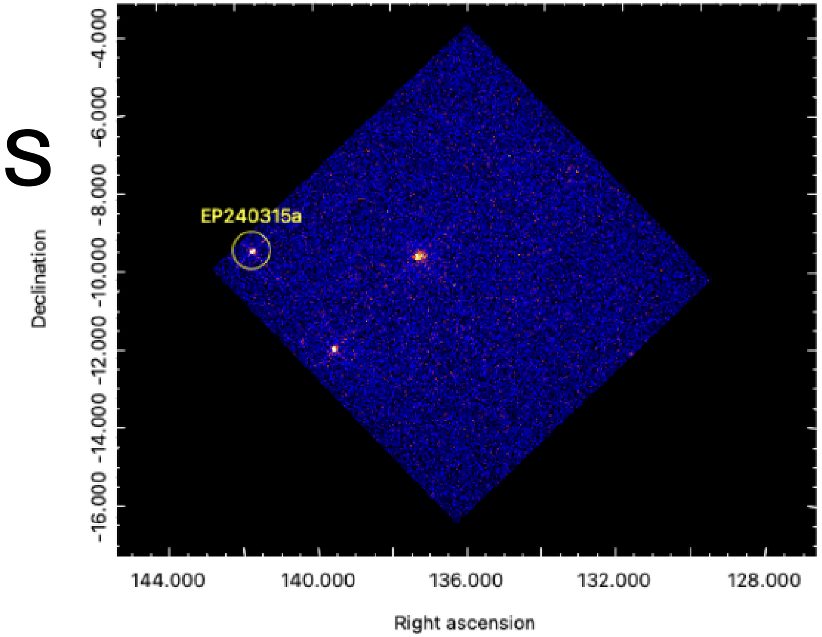

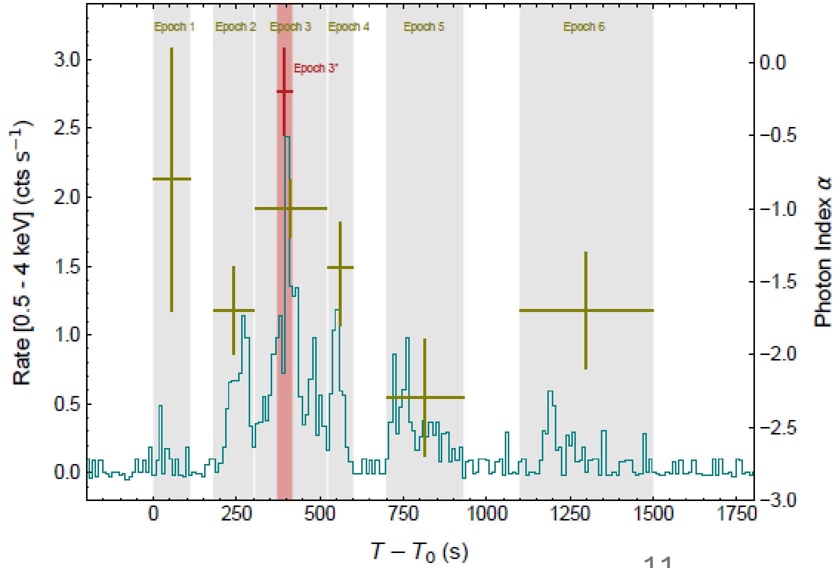

Ep240315a / GRB 240315C. Liu+ 2014, arXiv:2404.16425

What is currently happening in our field?

A list of noteworthy recent GRBs

- GRB 160821B. Short GRB with TeV emission.
- GRB 170817A. gravitational waves detected.
- GRB 180720B. HESS detected.
- GRB 190114C. TeV photons MAGIC.
- GRB 190829A. TeV photons.
- GRB 200826A. A short GRB from massive star collapse.
- GRB 201015A. TeV burst.
- GRB 201216C. MAGIC detected.
- GRB 210610B. 54 deg polarization angle rotation.
- GRB 211211A. long GRB from neutron star merger.
- GRB 221009A. brightest of all time.
- GRB 230307A. long GRB with a kilonova.
- GRB 240219A. Einstein Probe detection EP240219A.
- GRB 240315C. Einstein Probe detection.
- GRB 240402B. LEIA detection.

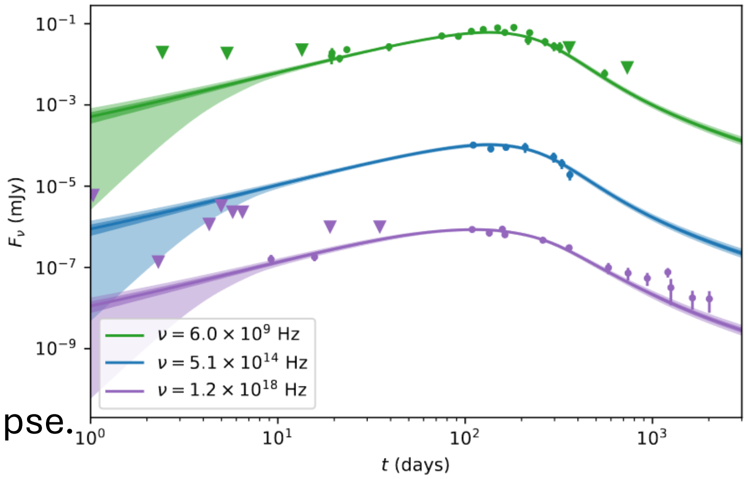

Ryan, van Eerten et al. 2023, ArXiv:2310.02328

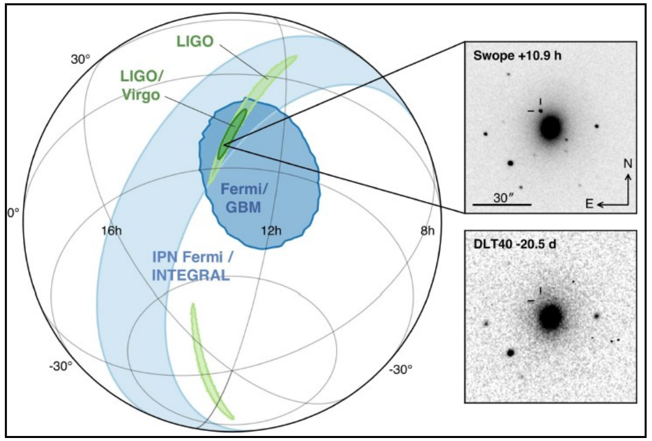

Abbott+ 2017

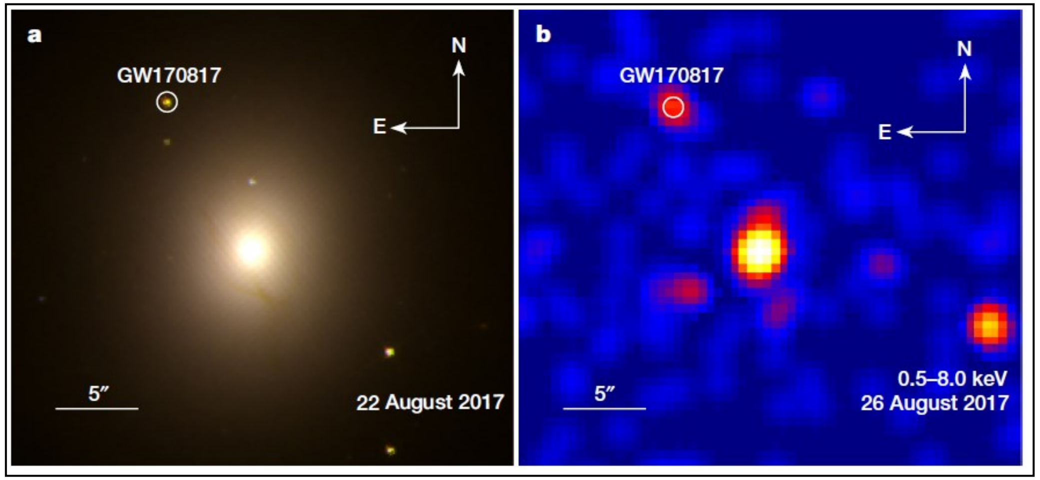

Troja, Piro, Van Eerten+ 2017

Observing a GRB afterglow jet at an angle

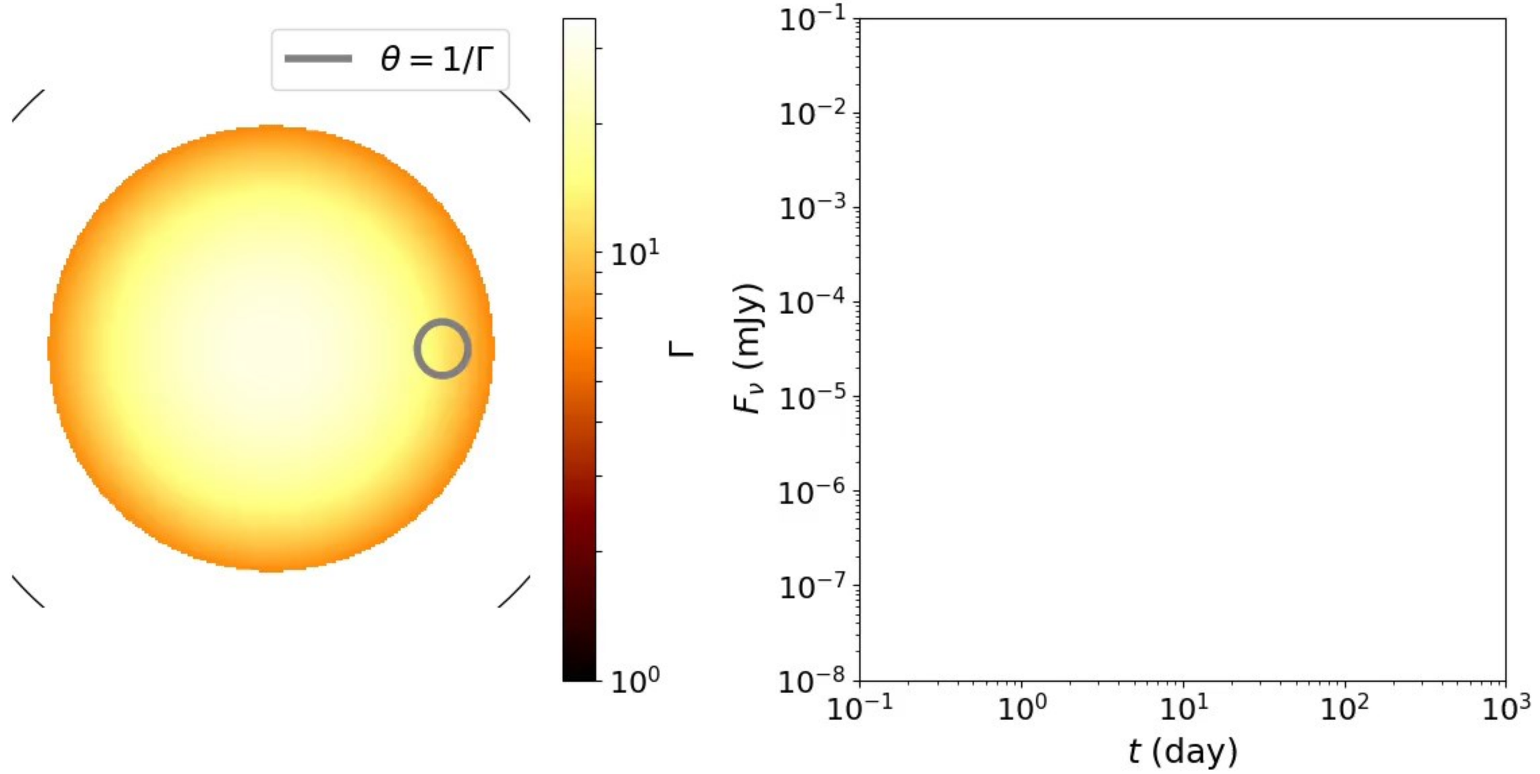

Ryan, HJvE+ 2020, ApJ 896, 166

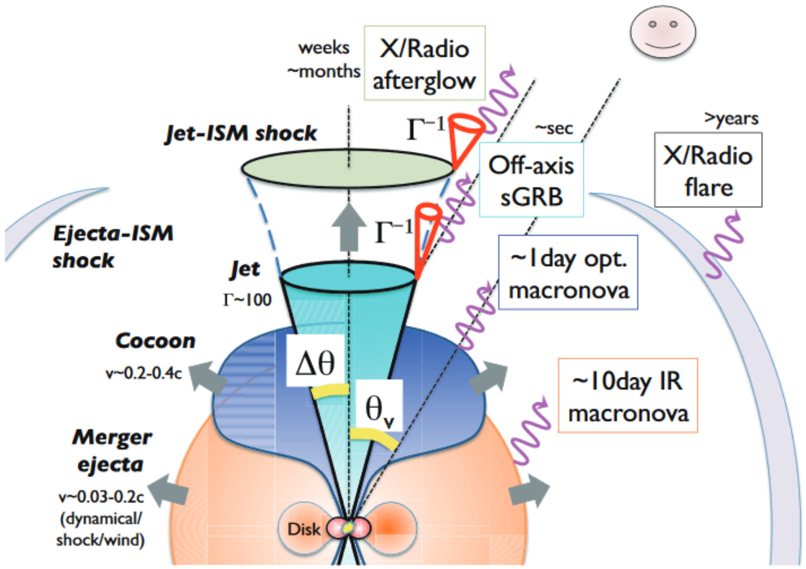

Ioka & Nakamura 2018, Prog Th. Exp. Phys 043E02

Without detailed modelling: merely looking at centroid and light curve slope

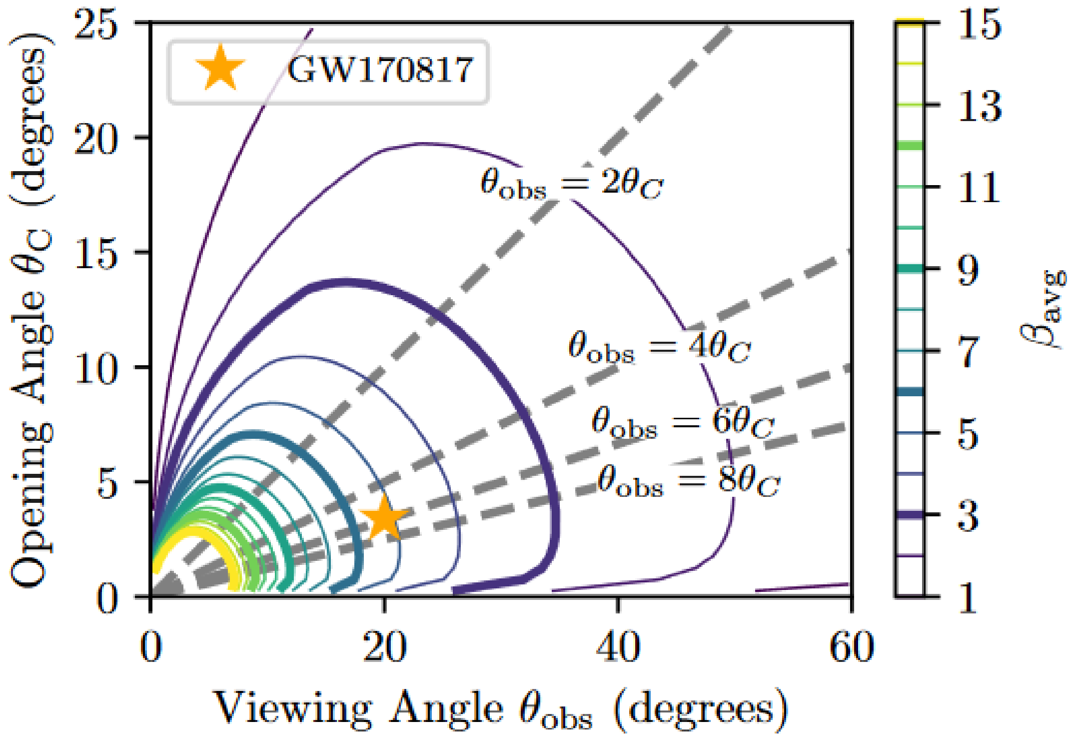

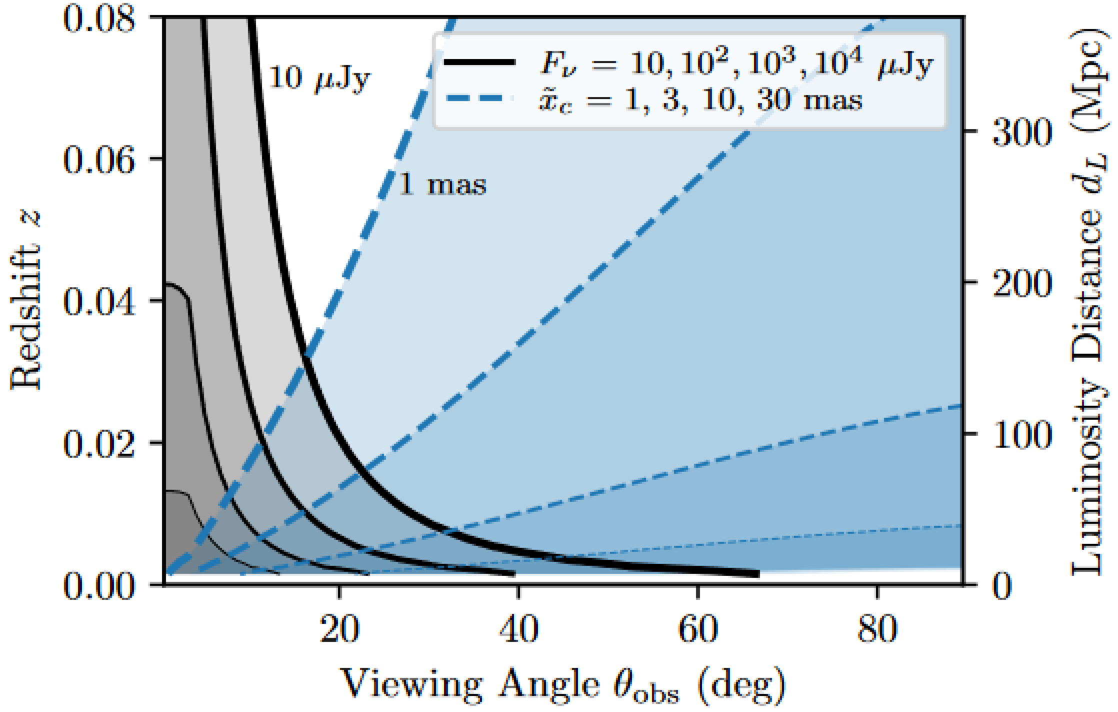

Ryan, Van Eerten, Troja, Piro, O'Connor & Ricci, ArXiv: 2310.02328

a single rising slope measurement *plus* centroid velocity suffice to determine jet orientation *and* opening angle

for context, the expected flux and centroid offset at peak time (jet break) for a GRB 170817-type event

approach exploits scale-invariance synchrotron transients, see e.g. Van Eerten & Ryan 2024, MNRAS 530, 4094

full long term modelling with *afterglowpy*

A publicly available python tool for quickly generating afterglow light curves for choice of physics parameters
Ryan, Van Eerten, Piro, Troja 2020, ApJ 896, 166
https://github.com/geoffryan/afterglowpy
“pip install afterglowpy”

- Based on a shell model, calibrated to simulations.
- synchrotron radiation from integrating over emission surface
- various jet structures & choked jet models
- couples easily to e.g. Emcee (Foreman-Mackey+ 2013)

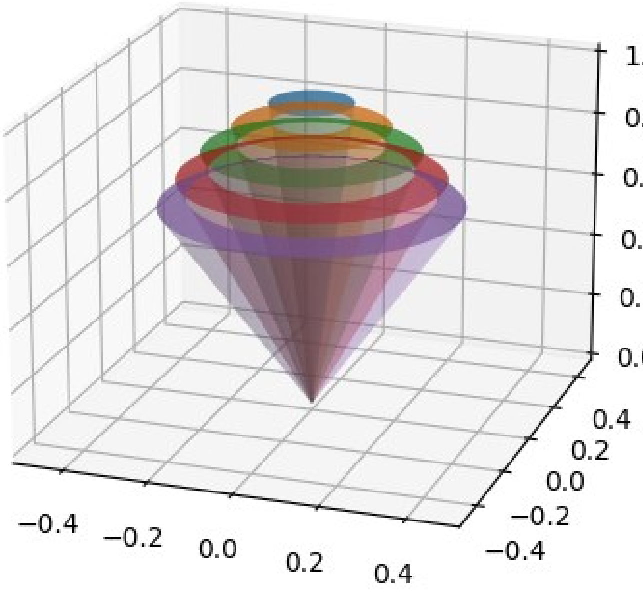

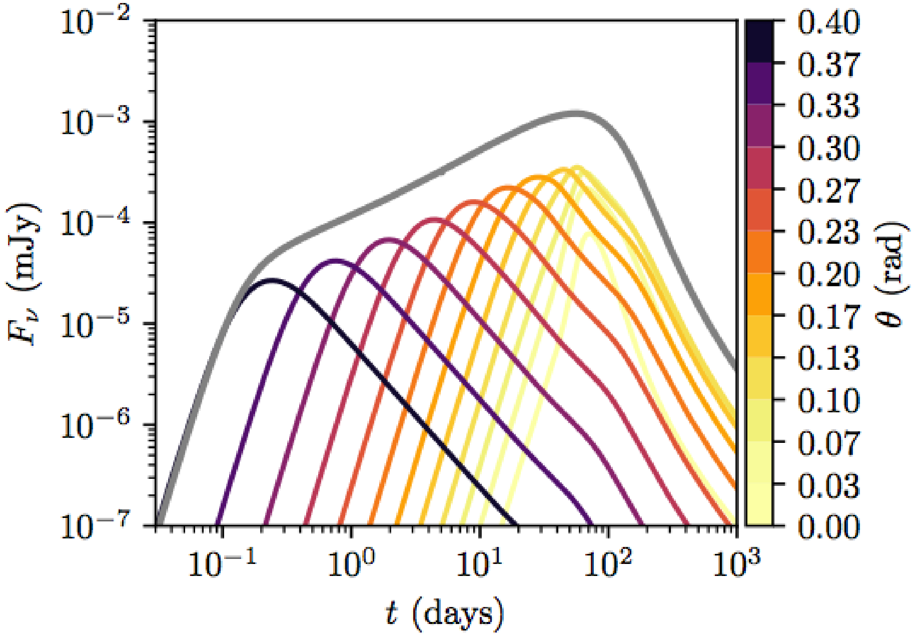

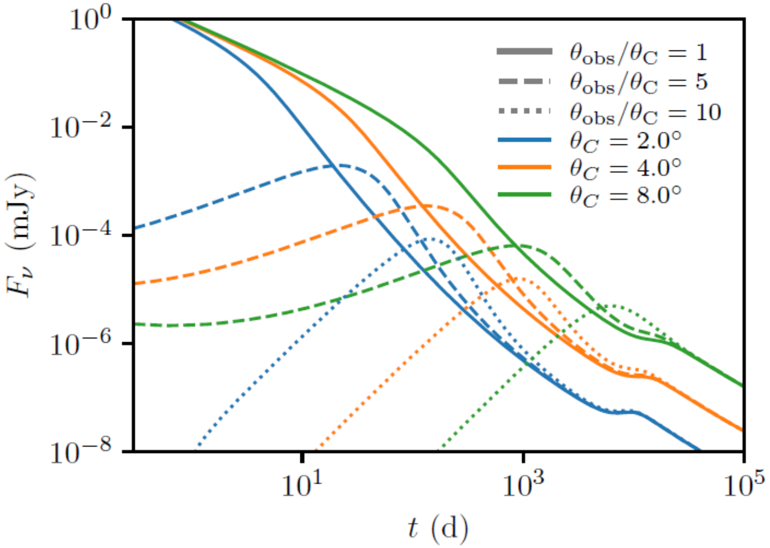

Similar tools ‘on the market’:
jetsimpy, Wang+ 2024, arXiv:2402.19359
JEDI, Lu+ 2020, arXiv:2005.10313

Feature updates afterglowpy

Ryan, Van Eerten, Troja, Piro, O'Connor & Ricci, ArXiv: 2310.02328
afterglowpy v0.8 now public

- Deep Newtonian limit
  Huang & Cheng 2003; Granot+ 2006; Sironi & Giannios 2013
- Centroid motion and image on sky

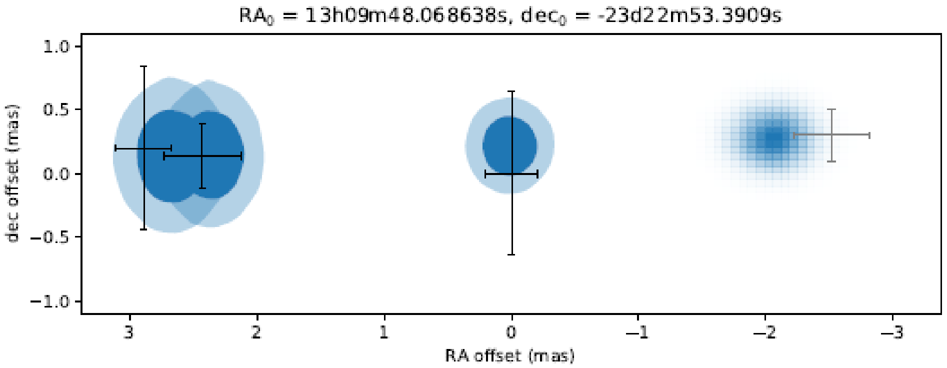

data from Ghirlanda+ 2019, Mooley+ 2018, 2022

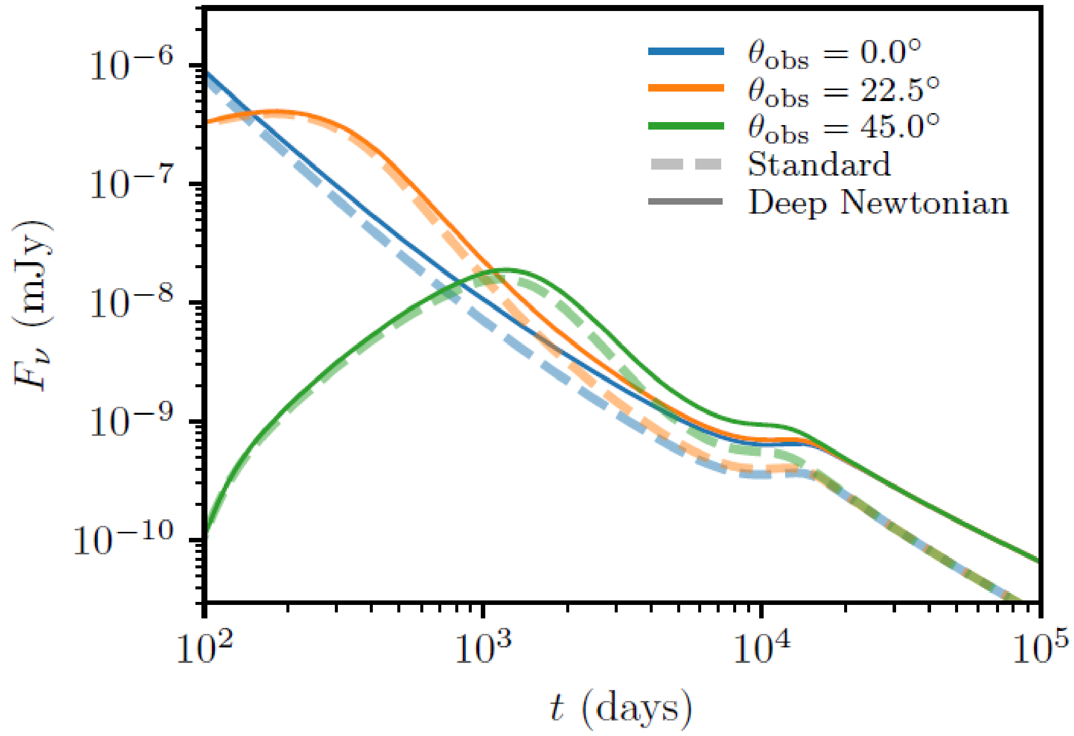

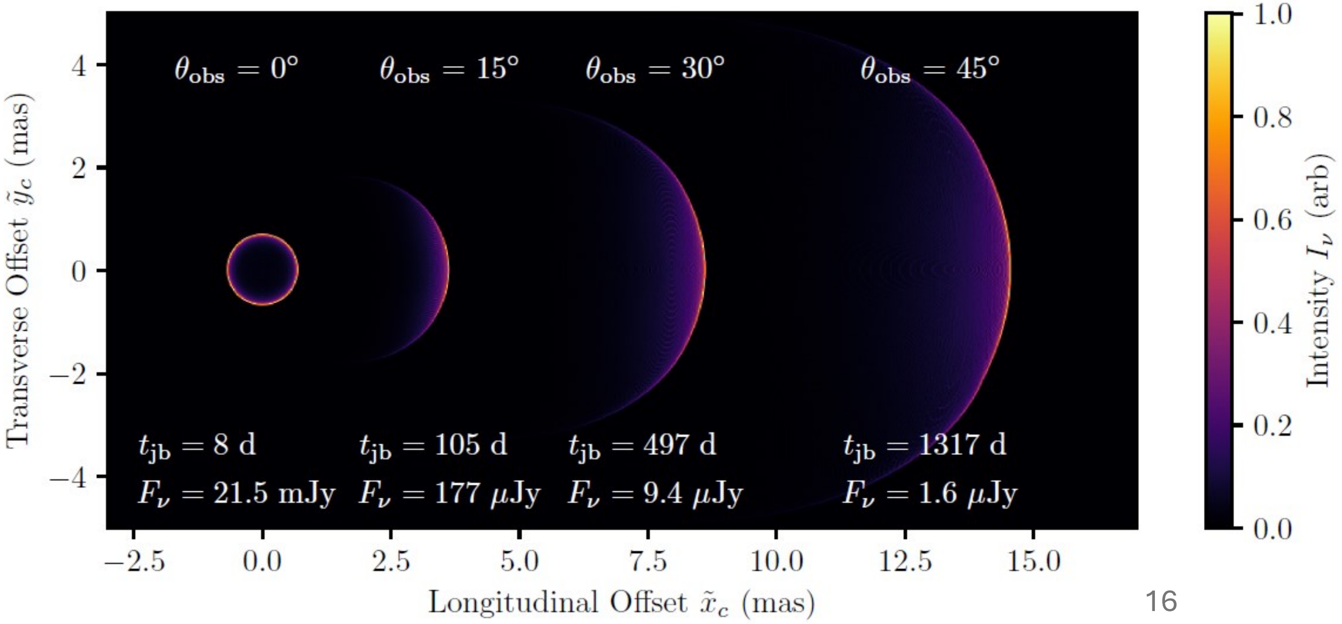

Full Bayesian *afterglowpy* modelling of GRB 170817A

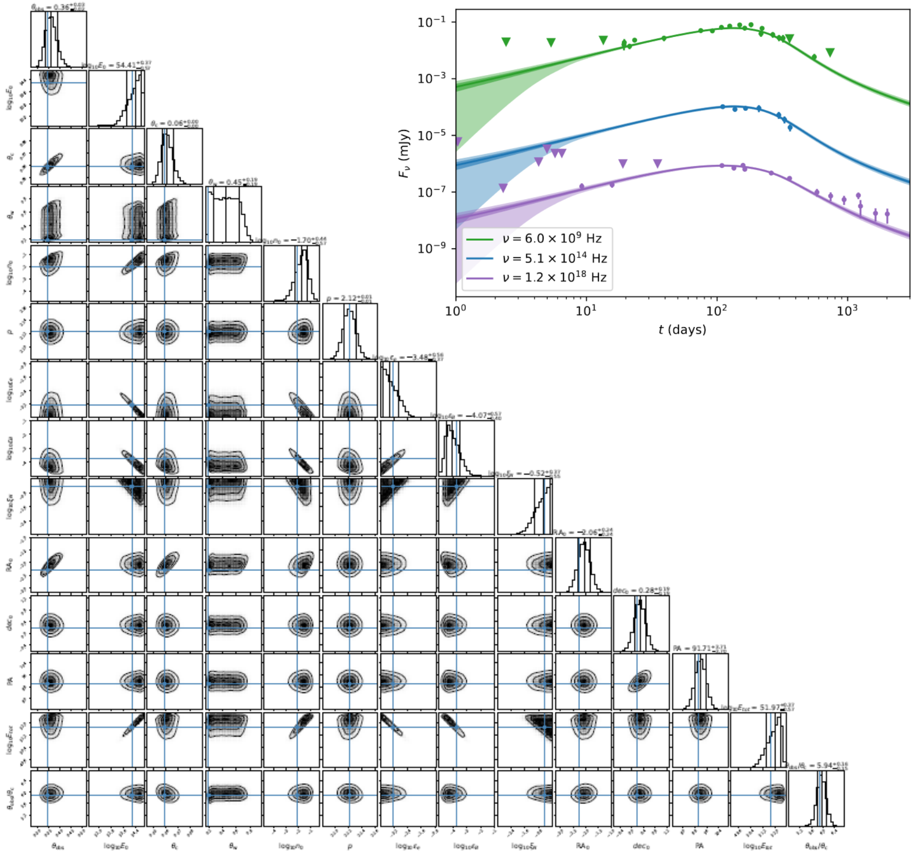

to actually read those numbers, see:
Ryan, van Eerten et al. 2023, ArXiv:2310.02328

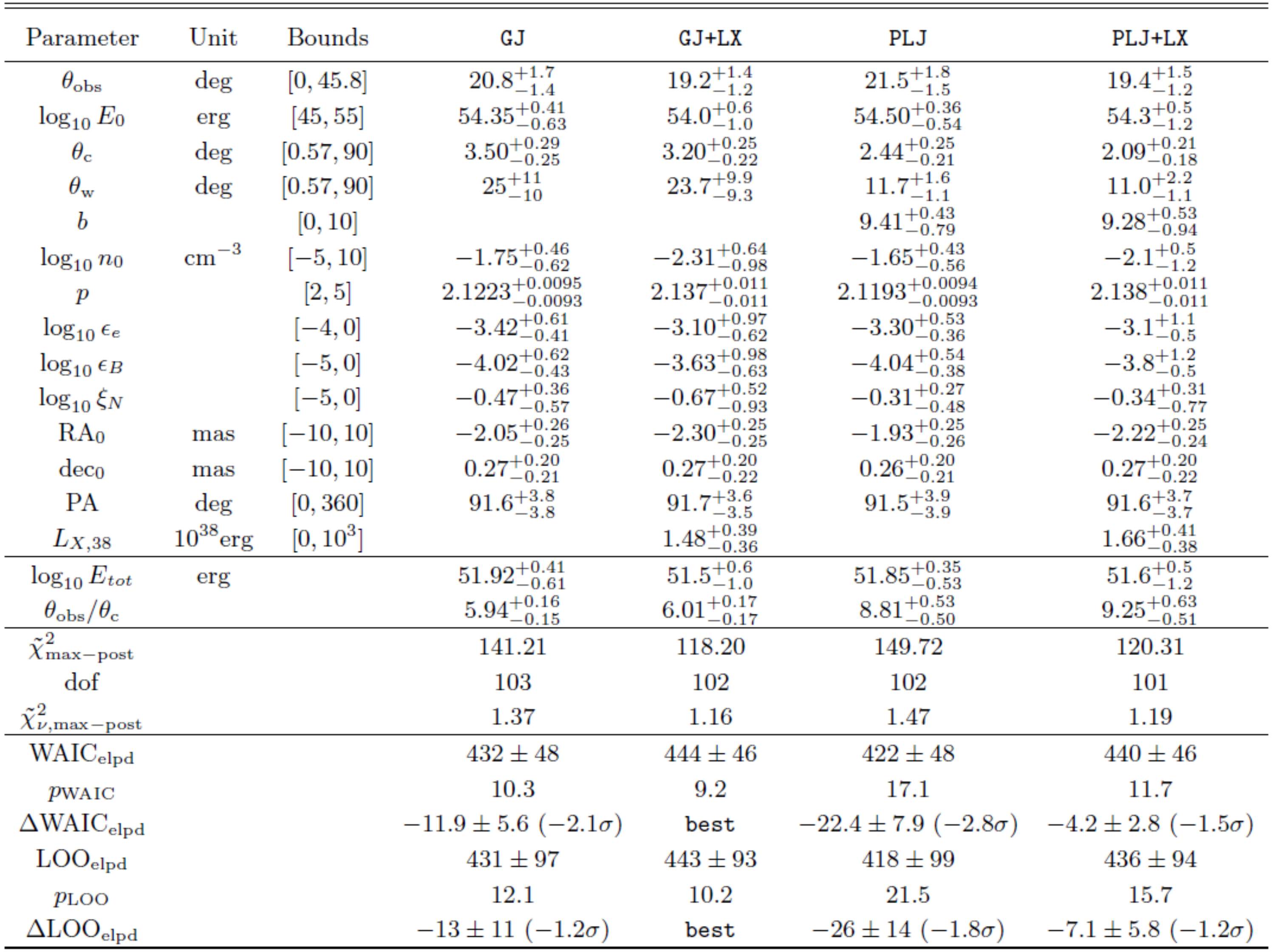

Parameter	Unit	Bounds	GJ	GJ+LX	PLJ	PLJ+LX
$\theta_{\rm obs}$	deg	$[0, 45.8]$	$20.8^{+1.7}_{-1.4}$	$19.2^{+1.4}_{-1.2}$	$21.5^{+1.8}_{-1.5}$	$19.4^{+1.5}_{-1.2}$
$\log_{10} E_0$	erg	$[45, 55]$	$54.35^{+0.41}_{-0.63}$	$54.0^{+0.6}_{-1.0}$	$54.50^{+0.36}_{-0.54}$	$54.3^{+0.5}_{-1.2}$
$\theta_{\rm c}$	deg	$[0.57, 90]$	$3.50^{+0.29}_{-0.25}$	$3.20^{+0.25}_{-0.22}$	$2.44^{+0.25}_{-0.21}$	$2.09^{+0.21}_{-0.18}$
$\theta_{\rm w}$	deg	$[0.57, 90]$	25^{+11}_{-10}	$23.7^{+9.9}_{-9.3}$	$11.7^{+1.6}_{-1.1}$	$11.0^{+2.2}_{-1.1}$
b		$[0, 10]$			$9.41^{+0.43}_{-0.79}$	$9.28^{+0.53}_{-0.94}$
$\log_{10} n_0$	cm^{-3}	$[-5, 10]$	$-1.75^{+0.46}_{-0.62}$	$-2.31^{+0.64}_{-0.98}$	$-1.65^{+0.43}_{-0.56}$	$-2.1^{+0.5}_{-1.2}$
p		$[2, 5]$	$2.1223^{+0.0095}_{-0.0093}$	$2.137^{+0.011}_{-0.011}$	$2.1193^{+0.0094}_{-0.0093}$	$2.138^{+0.011}_{-0.011}$
$\log_{10} \epsilon_e$		$[-4, 0]$	$-3.42^{+0.61}_{-0.41}$	$-3.10^{+0.97}_{-0.62}$	$-3.30^{+0.53}_{-0.36}$	$-3.1^{+1.1}_{-0.5}$
$\log_{10} \epsilon_B$		$[-5, 0]$	$-4.02^{+0.62}_{-0.43}$	$-3.63^{+0.98}_{-0.63}$	$-4.04^{+0.54}_{-0.38}$	$-3.8^{+1.2}_{-0.5}$
$\log_{10} \xi_N$		$[-5, 0]$	$-0.47^{+0.36}_{-0.57}$	$-0.67^{+0.52}_{-0.93}$	$-0.31^{+0.27}_{-0.48}$	$-0.34^{+0.31}_{-0.77}$
RA_0	mas	$[-10, 10]$	$-2.05^{+0.26}_{-0.25}$	$-2.30^{+0.25}_{-0.25}$	$-1.93^{+0.25}_{-0.26}$	$-2.22^{+0.25}_{-0.24}$
dec_0	mas	$[-10, 10]$	$0.27^{+0.20}_{-0.21}$	$0.27^{+0.20}_{-0.22}$	$0.26^{+0.20}_{-0.21}$	$0.27^{+0.20}_{-0.22}$
PA	deg	$[0, 360]$	$91.6^{+3.8}_{-3.8}$	$91.7^{+3.6}_{-3.5}$	$91.5^{+3.9}_{-3.9}$	$91.6^{+3.7}_{-3.7}$
$L_{X,38}$	10^{38}erg	$[0, 10^3]$		$1.48^{+0.39}_{-0.36}$		$1.66^{+0.41}_{-0.38}$
$\log_{10} E_{tot}$	erg		$51.92^{+0.41}_{-0.61}$	$51.5^{+0.6}_{-1.0}$	$51.85^{+0.35}_{-0.53}$	$51.6^{+0.5}_{-1.2}$
$\theta_{\rm obs}/\theta_{\rm c}$			$5.94^{+0.16}_{-0.15}$	$6.01^{+0.17}_{-0.17}$	$8.81^{+0.53}_{-0.50}$	$9.25^{+0.63}_{-0.51}$
$\tilde{\chi}^2_{\rm max-post}$			141.21	118.20	149.72	120.31
dof			103	102	102	101
$\tilde{\chi}^2_{\nu,\rm max-post}$			1.37	1.16	1.47	1.19
$\mathrm{WAIC}_{\rm elpd}$			432 ± 48	444 ± 46	422 ± 48	440 ± 46
$p_{\rm WAIC}$			10.3	9.2	17.1	11.7
$\Delta\mathrm{WAIC}_{\rm elpd}$			-11.9 ± 5.6 (-2.1σ)	best	-22.4 ± 7.9 (-2.8σ)	-4.2 ± 2.8 (-1.5σ)
$\mathrm{LOO}_{\rm elpd}$			431 ± 97	443 ± 93	418 ± 99	436 ± 94
$p_{\rm LOO}$			12.1	10.2	21.5	15.7
$\Delta\mathrm{LOO}_{\rm elpd}$			-13 ± 11 (-1.2σ)	best	-26 ± 14 (-1.8σ)	-7.1 ± 5.8 (-1.2σ)

The impact of various model aspects

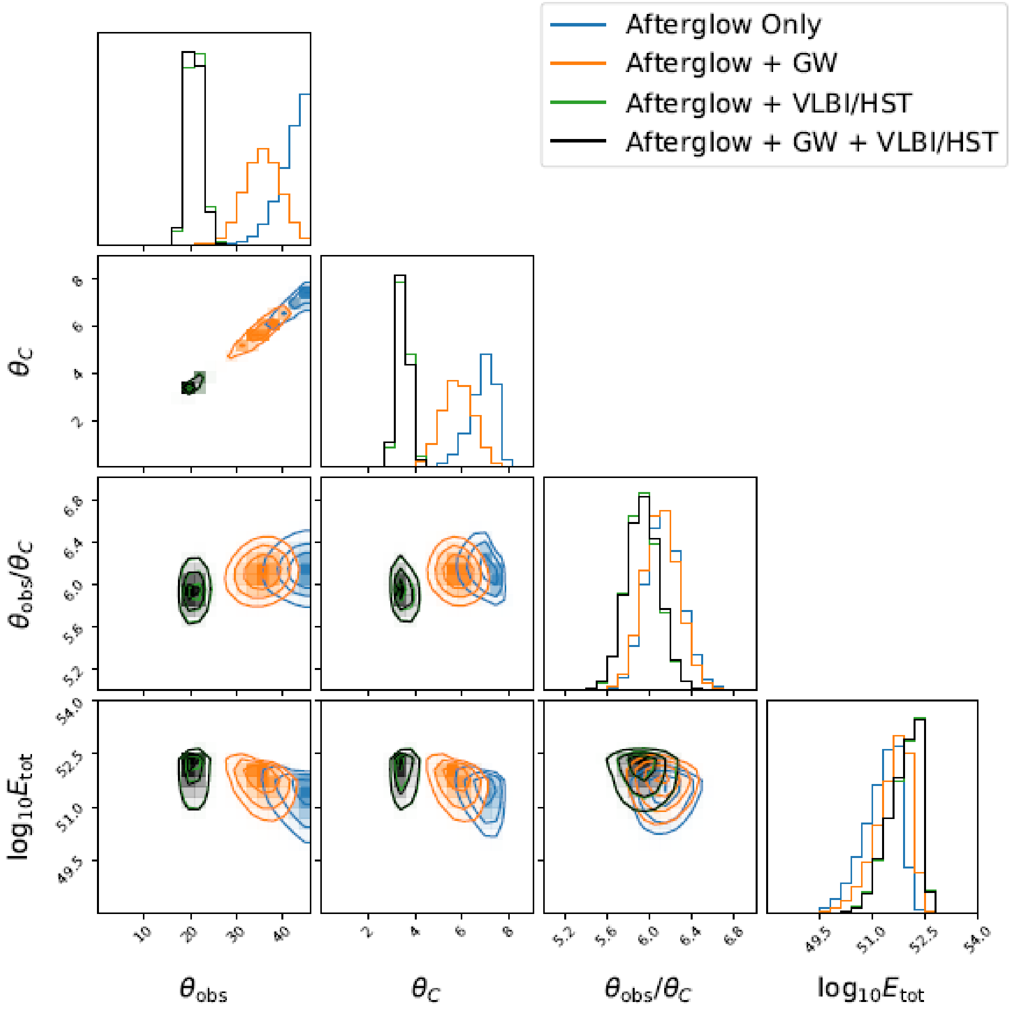

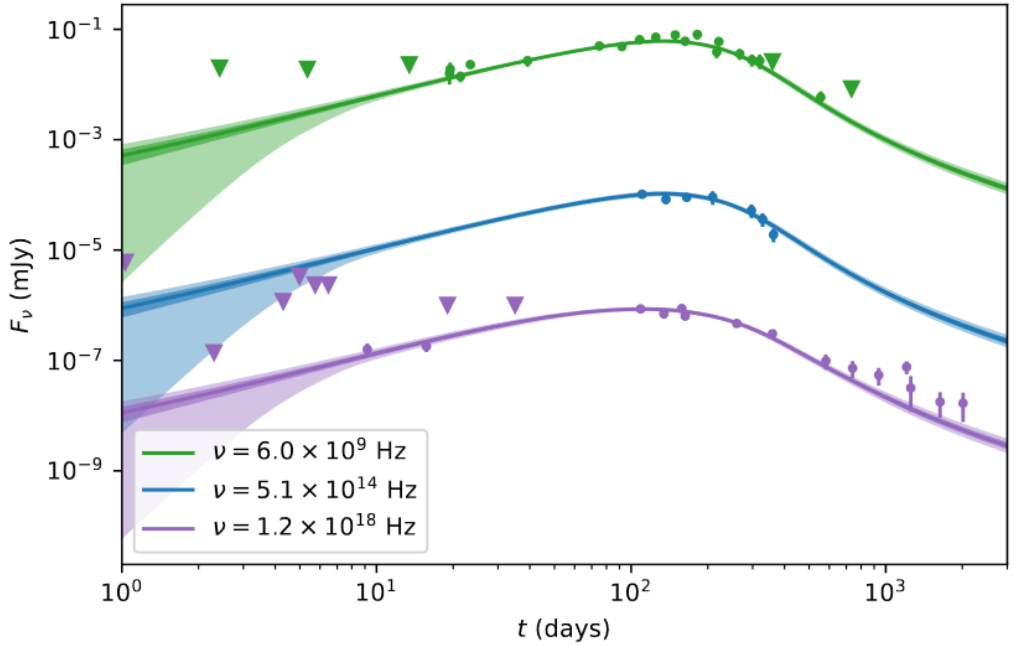

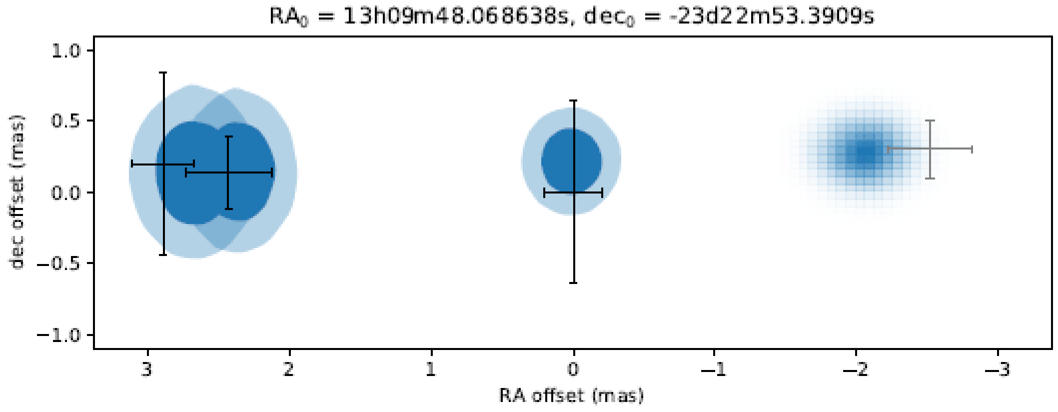

Ryan, van Eerten et al. 2023, ArXiv:2310.02328

The impact of various model aspects

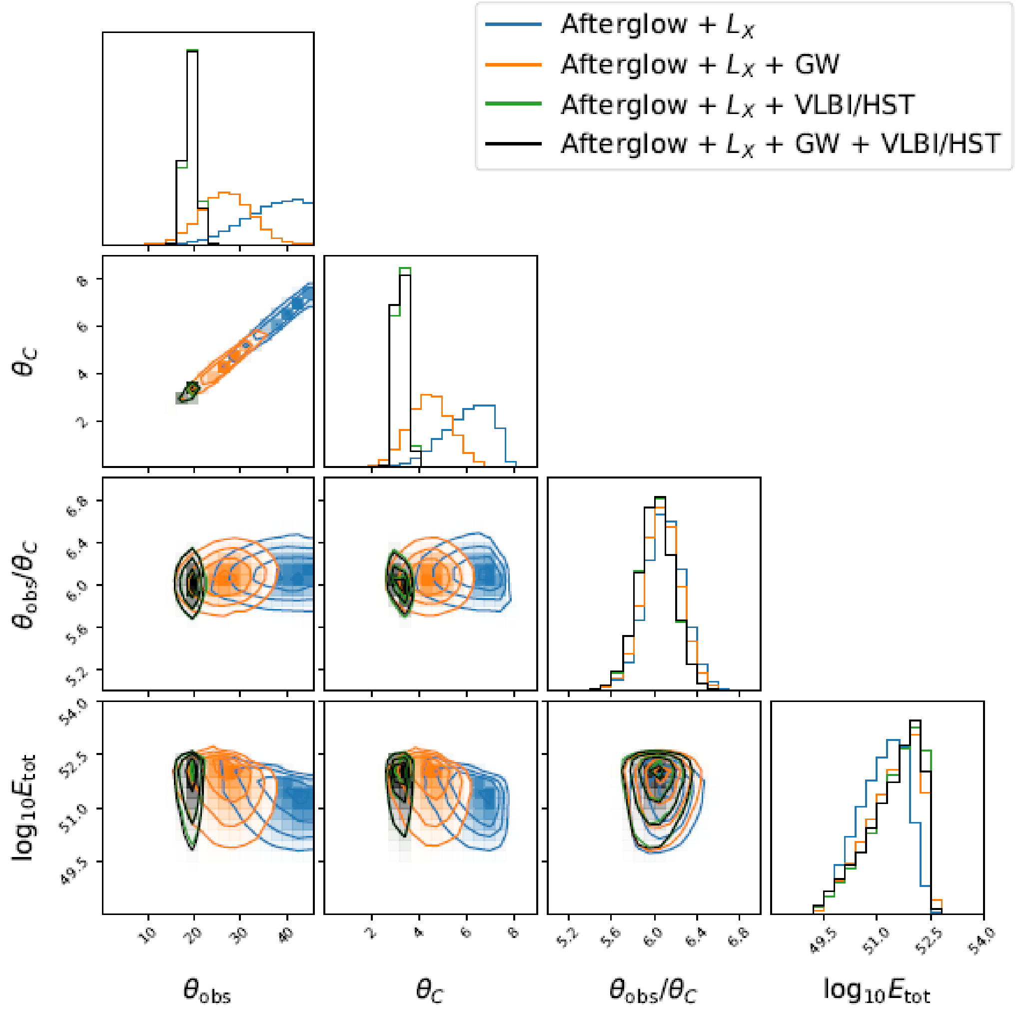

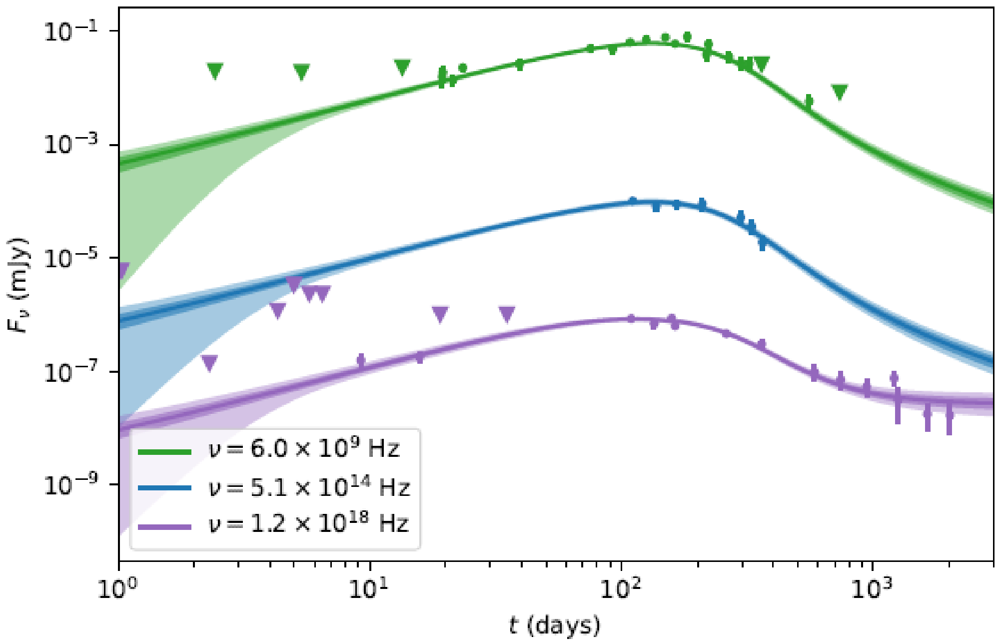

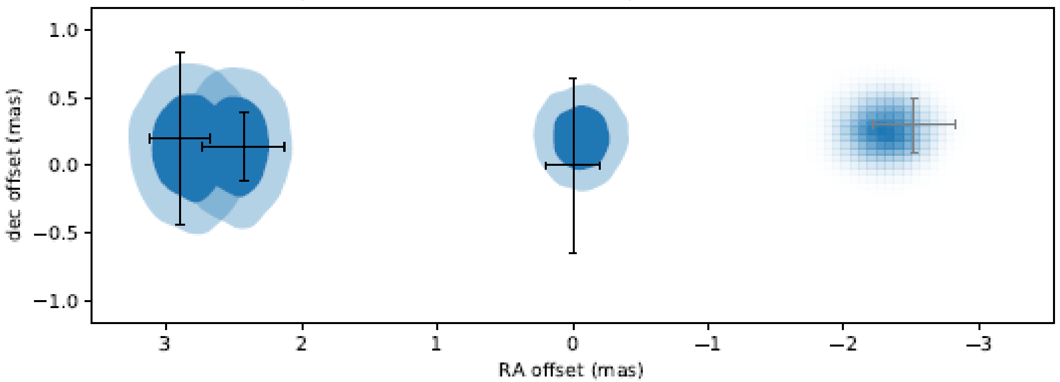

Adding extra X-ray luminosity helps, but not statistically required (2.1 sigma improvement)

Ryan, van Eerten et al. 2023, ArXiv:2310.02328

Best fit "versus" Bayesian statistics

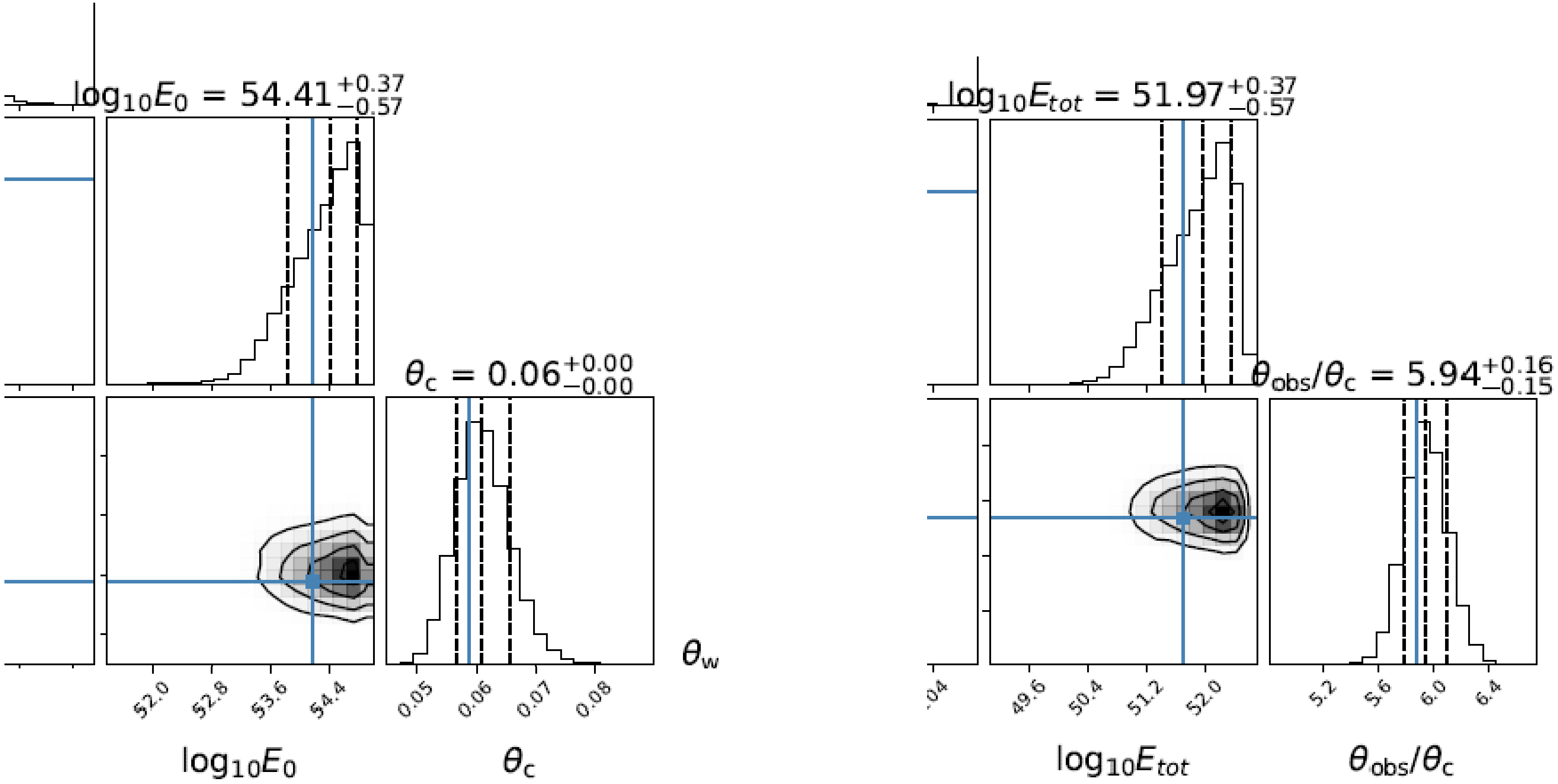

Ryan, van Eerten et al. 2023, ArXiv:2310.02328

Is that not too much energy?

Best fit “versus” Bayesian statistics

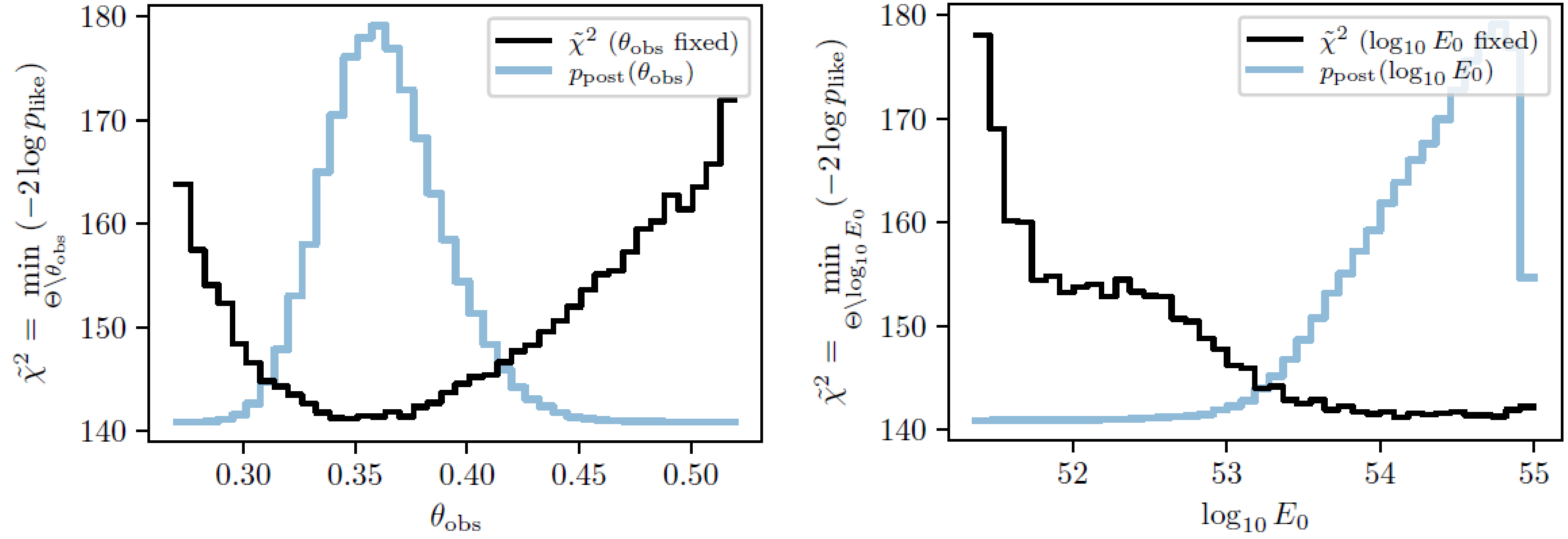

Left: example of well-constrained variable (jet orientation)

Right: example of broad range for variable (jet energy)

Ryan, van Eerten et al. 2023, ArXiv:2310.02328

$$P(\Theta|D, M) = \frac{P(D|\Theta, M)P(\Theta|M)}{P(D|M)}$$

The *prior* belief in our parameter distribution Θ is $P(\Theta|M)$

The *evidence* for a given model *M* is $P(D|M) = \int P(D|\Theta, M)P(\Theta|M)d\Theta$

For a given parameter θ_1 we have a posterior probability $P(\theta_1|D, M) = \int P(\Theta|D, M)d\theta_2 d\theta_3 \ldots d\theta_N$

Summary

- **Gamma-ray burst jets are formed during brief period of accretion on newly formed black hole (or temporary or durable magnetar).**
- **Both long and short GRB “jets” have structure following launch.**
- **GRB 170817 still visible in X-rays, some tension with jet models due to higher-than-expected brightness.**
- **Multiple recent bursts are seemingly at odds with the long (collapsar & supernova) / short (merging neutron stars & kilonova) divide.**
- **Since 2019, a growing sample of TeV-detected afterglows (7, both long and short, detected by MAGIC, H.E.S.S., LHAASO).**
- **GRB 221009A, the “BOAT” blows all previous GRBs out of the water. Has TeV-detections, polarization, sky-imaging and a broad lateral structured jet.**
- ***Afterglowpy* has been updated to include the “Deep Newtonian” radiation regime and sky images / centroid motion.**

Many open questions in the field:

- How can a neutron-star merger produce a GRB prompt stage well longer than 2 s, in view of expected accretion time scales?
- What jet structure *(lateral distribution of energy*) is imposed by accretion disk, neutrino-driven wind and merger ejecta?
- Can TeV-emission from GRB jets be reconciled with synchrotron component? SSC or other sites of seed photons?
- What explains the jet structure of the BOAT? And its light curves more generally?
- Are the latest trends in GRB 170817A (GW170817) observations compatible with a “standard” jet model or showing additional components?
- What causes soft X-rays in Einstein Probe-detected GRB 240315C? Are there going to be many more of these, continuously connecting to XRFs (X-ray flares) population?
- Those, and the classics: *How are GRB jets launched? How do GRB shocks accelerate particles? Can NS-BH mergers or other merger types trigger GRB jets? Do GRB jets contribute to cosmic rays and/or extra-galactic neutrinos? etc..*

extra slides

Afterglows are the mainstream tool to constrain jet features

- parameters associated with the environment
  circumburst density scale A (ρ_{ext}); density radial slope k, $\rho_{ext} \propto r^{-k}$
- parameters associated with the jet
  energy in the jet E (E_{iso}); energy injection temporal slope q, $E \propto t^{-q}$
  jet opening angle(s) θ_0 (θ_c, θ_w); other jet structure parameters b
- parameters associated with the radiative process
  energy fraction in non-thermal electrons ε_e
  participation fraction non-thermal electrons ξ_N
  energy fraction in the magnetic field ε_B
  slope of non-thermal electron distribution p
- parameters associated with the observer
  jet orientation θ_{obs}, redshift z, luminosity distance d_L

Note, not all parameters used / needed at all times

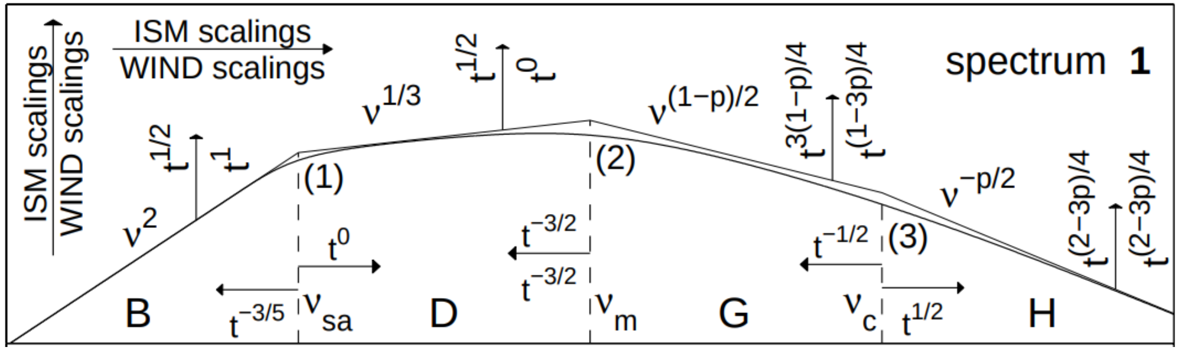

Granot & Sari 2002, ApJ 568, 820

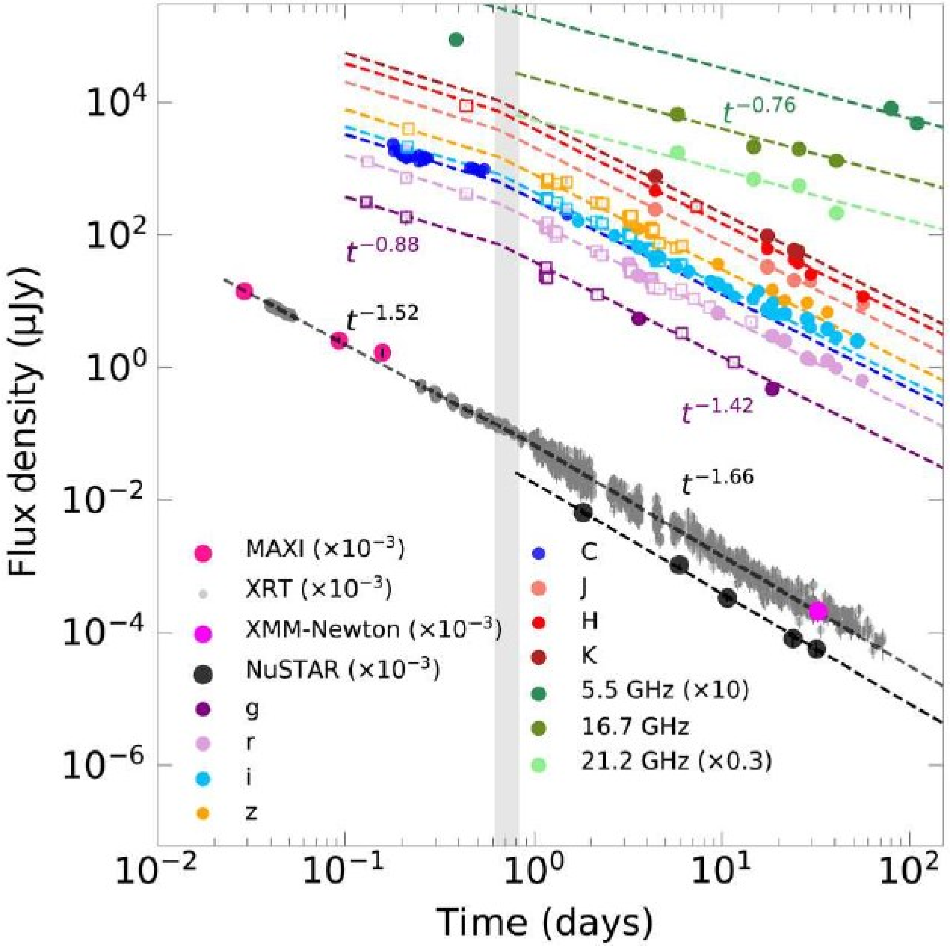

O'Connor+ 2023
Science Advances 9, 1405

dynamics basics, shell model

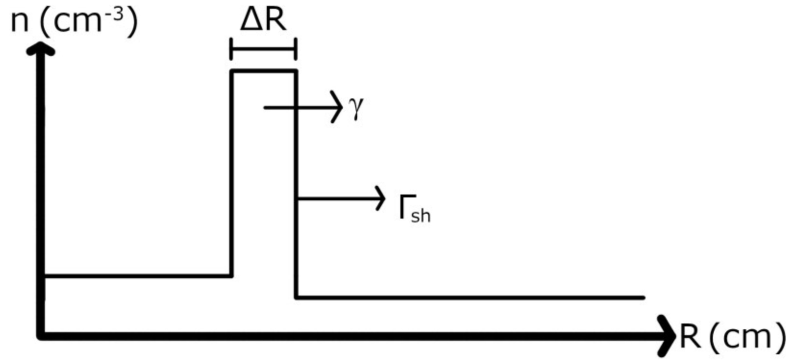

$$E_{iso} = (\gamma - 1) M_{ej} c^2 + \frac{\beta^2}{3}(4\gamma^2 - 1) M_{sw} c^2$$

$$\frac{1}{\gamma^2}\frac{d\gamma^2}{dt} \cong \frac{1}{M_{sw}}\frac{dM_{sw}}{dt}$$

$$\frac{dM_{sw}}{dt} = 4\pi\rho_{ext} R^2 \frac{dR}{dt}$$

$$\frac{dR}{dt} = c\beta \cong c\left(1 - \frac{1}{2\gamma^2}\right)$$

Piran 1999; Pe’er 2012; HJvE 2013; Nava 2013

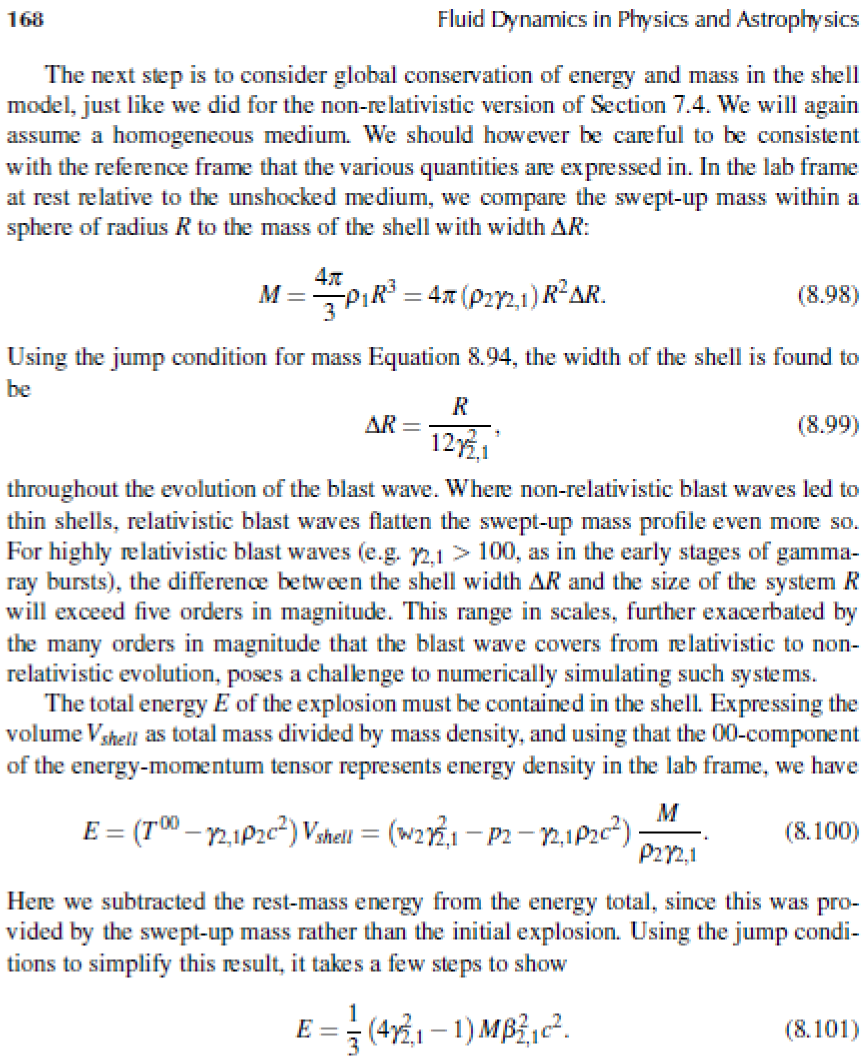

168 Fluid Dynamics in Physics and Astrophysics

The next step is to consider global conservation of energy and mass in the shell model, just like we did for the non-relativistic version of Section 7.4. We will again assume a homogeneous medium. We should however be careful to be consistent with the reference frame that the various quantities are expressed in. In the lab frame at rest relative to the unshocked medium, we compare the swept-up mass within a sphere of radius R to the mass of the shell with width ΔR:

$$M = \frac{4\pi}{3}\rho_1 R^3 = 4\pi\left(\rho_2 \gamma_{2,1}\right) R^2 \Delta R. \qquad (8.98)$$

Using the jump condition for mass Equation 8.94, the width of the shell is found to be

$$\Delta R = \frac{R}{12\gamma_{2,1}^2}, \qquad (8.99)$$

throughout the evolution of the blast wave. Where non-relativistic blast waves led to thin shells, relativistic blast waves flatten the swept-up mass profile even more so. For highly relativistic blast waves (e.g. $\gamma_{2,1} > 100$, as in the early stages of gamma-ray bursts), the difference between the shell width ΔR and the size of the system R will exceed five orders in magnitude. This range in scales, further exacerbated by the many orders in magnitude that the blast wave covers from relativistic to non-relativistic evolution, poses a challenge to numerically simulating such systems.

The total energy E of the explosion must be contained in the shell. Expressing the volume V_{shell} as total mass divided by mass density, and using that the 00-component of the energy-momentum tensor represents energy density in the lab frame, we have

$$E = \left(T^{00} - \gamma_{2,1}\rho_2 c^2\right) V_{shell} = \left(w_2 \gamma_{2,1}^2 - p_2 - \gamma_{2,1}\rho_2 c^2\right) \frac{M}{\rho_2 \gamma_{2,1}}. \qquad (8.100)$$

Here we subtracted the rest-mass energy from the energy total, since this was provided by the swept-up mass rather than the initial explosion. Using the jump conditions to simplify this result, it takes a few steps to show

$$E = \frac{1}{3}\left(4\gamma_{2,1}^2 - 1\right) M \beta_{2,1}^2 c^2. \qquad (8.101)$$

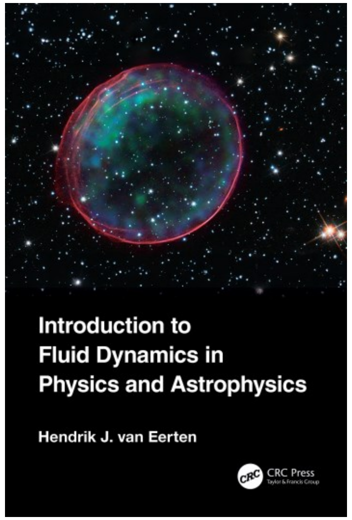

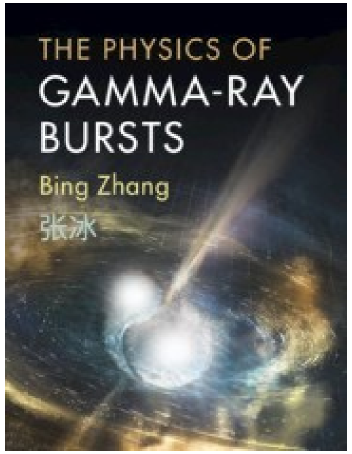

there are many studies covering GRB 170817

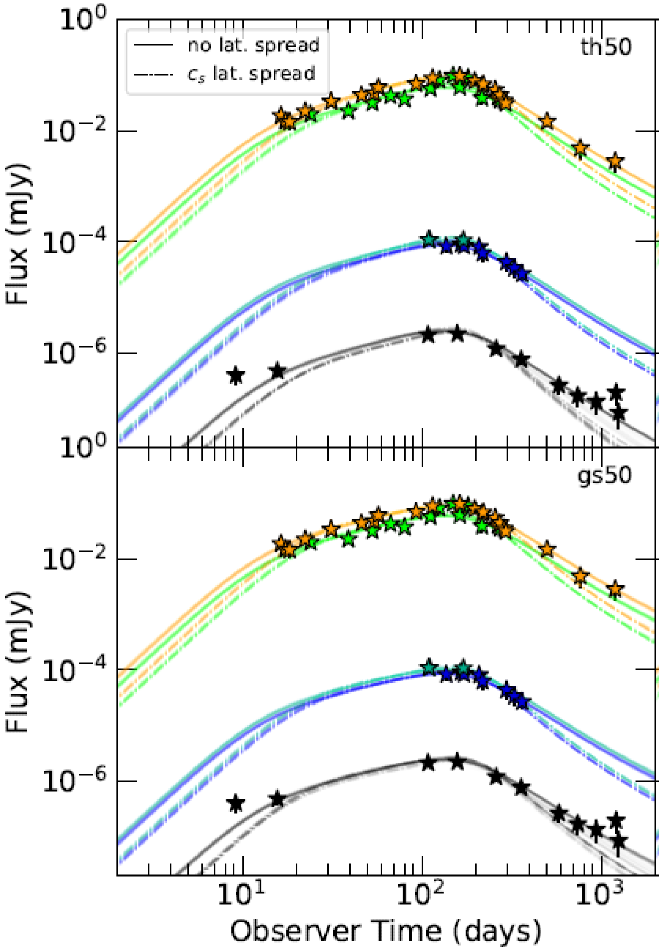

Nativi+ 2022, MNRAS

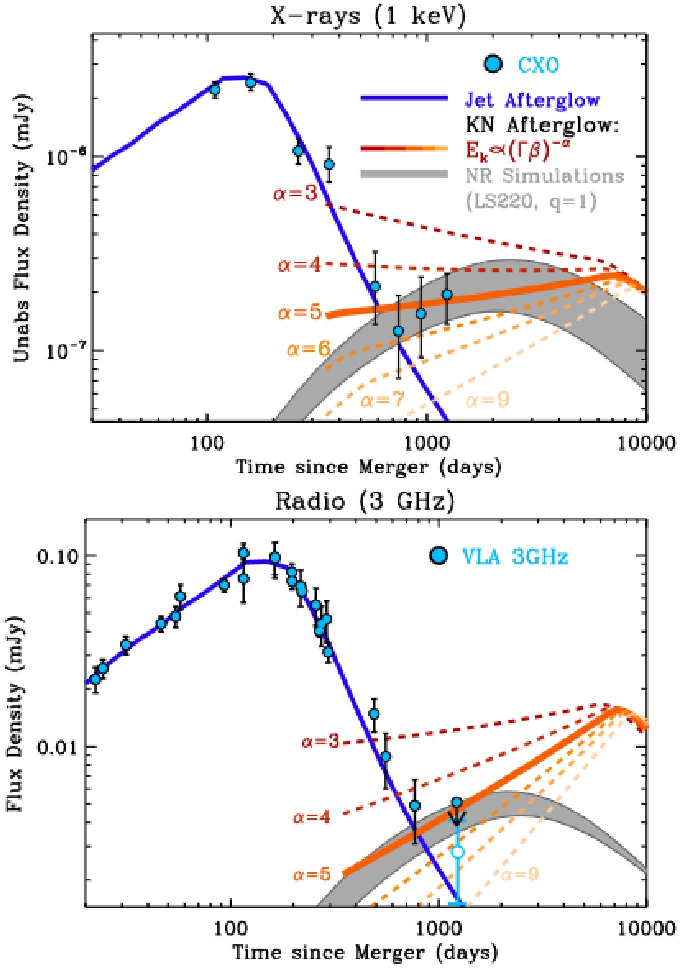

Hajela+ 2022 APJL 502, 1843

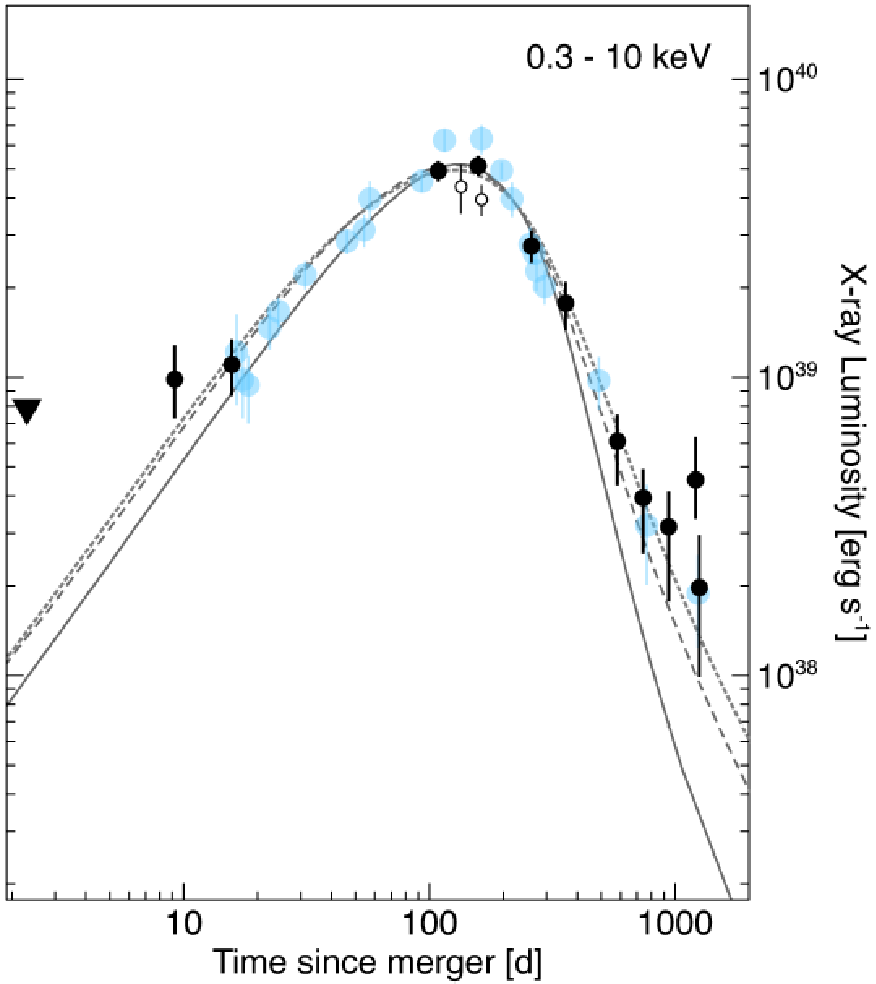

Troja+ 2022

Katu – The Kinetic Equation (spectrum slide 6)

Adiabatic expansion

IC cooling (w/ Klein Nishina)

$$\frac{\partial n}{\partial t} = \mathcal{Q}_e + \mathcal{Q}_i + \mathcal{L} - \frac{n}{\tau_{esc}} - \frac{n}{\tau_{dec}} - \frac{\partial}{\partial \gamma}\left(\frac{\partial \gamma}{\partial t} n\right)$$

Particles gained/lost overall

External injection

Internal injection

Internal losses

Escaped particles

Decaying particles

Synchrotron/IC gains & losses

Hope, van Eerten & Schady, in prep.

Standard Jet test from slide 6

- **E_0 = 1e53**
- b = 2 (Power-law only)
- $\theta_c = 0.08$
- $\theta_w = 0.24$
- n_0 = 1 cm^{-3}
- p = 2.2
- $\varepsilon_e = 10^{-1}$
- $\varepsilon_B = 10^{-2}$
- z = 0.5454 ($d_L = 10^{28}$ cm)

We consider:

Structure of Jet

Top-hat, Gaussian, Power-law

(~18 Zones)

Observer Angle

0, 0.5, 1, 1.5 [θ_{obs}/θ_w]

Ryan et al. 2020

Hope, van Eerten & Schady, in prep.